ISLANDING DETECTION FOR DISTRIBUTED GENERATION

A DISSERTATION

Submitted in partial fulfillment of the
requirements for the award of the degree
of
MASTER OF TECHNOLOGY
in
ELECTRICAL ENGINEERING
(With specialization in Instrumentation and Signal Processing)

By

SANCHAY ADARI

DEPARTMENT OF ELECTRICAL ENGINEERING
INDIAN INSTITUTE OF TECHNOLOGY ROORKEE
ROORKEE - 247 667 (INDIA)
May 2016

CANDIDATE'S DECLARATION

I hereby declare that this thesis report entitled **ISLANDING DETECTION FOR DISTRIBUTED GENERATION**, submitted to the Department of Electrical Engineering, Indian Institute of Technology, Roorkee, India, in partial fulfillment of the requirements for the award of the Degree of Master of Technology in Electrical Engineering with specialization in Instrumentation and Signal Processing is an authentic record of the work carried out by me during the period June 2015 through May 2016, under the supervision of **Dr. BHAVESH BHALJA and Dr.MANOJ TRIPATHY, Department of Electrical Engineering, Indian Institute of Technology, Roorkee.** The matter presented in this thesis report has not been submitted by me for the award of any other degree of this institute or any other institutes.

Date:

Place: Roorkee

SANCHAY ADARI

CERTIFICATE

This is to certify that the above statement made by the candidate is true to the best of my knowledge and belief.

Dr. BHAVESH BHALJA
Associate Professor
Department of Electrical Engineering
Indian Institute of Technology Roorkee

Dr. MANOJ TRIPATHY Assista
Associate Professor
Department of Electrical Engineering
Indian Institute of Technology, Roorkee

ABSTRACT

This thesis presents two islanding detection techniques for distribution network having high penetration of Distributed Generations (DG's) system. Various islanding and non-islanding events for different values of active and reactive power mismatches are simulated using Real time digital simulator (RTDS) software. One of the proposed technique is based on the machine learning technique i.e and other technique is based on the passive islanding detection technique. The machine learning tool, Random forest technique is used as a classifier to classify the islanding events and the non-islanding events. The RF classifier utilizes sequence components of voltages which are obtained by acquiring voltage samples of all the phases from point of common coupling (PCC) of the targeted DG. The passive detection technque is based on the oscillation frequency of the synchronous generator. The change in the magnitude of the oscillation frequency is used to differentiate the islanding events from the non-islanding ones. Validity of the proposed schemes has been evaluated on large number of islanding/non-islanding cases which are generated by modeling standard IEEE 34-bus system for the technique based on Random forest classifier and by modelling standard IEEE 123 Bus System for the technique based on oscillation frequency of the synchronous generator. The simulation results indicate that the proposed schemes are capable to provide effective discrimination between islanding situation and non-islanding events. Moreover, they also gives satisfactory results during perfect power balance situation. In addition, it provides better stability in case of non-islanding events and hence, avoids nuisance tripping.

Acknowledgements

I would like to express my deep sense of gratitude and sincere thanks to my guide **Dr. Bhavesh Bhalja** and **Dr. Manoj Tripathy**, Department of Electrical Engineering, Indian Institute of Technology Roorkee, for their valuable guidance and support. I am highly indebted to them for their encouragement and constructive criticism throughout the course of this project work. Inspite of their hectic schedule, they were always there for clarifying my doubts and reviewed my dissertation progress in a constructive manner. Without their help, this thesis would not have been possible.

Also I would to thank Yogesh Makwana, Research Scholar, Department of Electrical Engineering for his help and support in understanding the project.

Sanchay Adari

Contents

List of Figures

List of Tables

Abbreviations

PCC	**P**oint of **C**ommon **C**oupling
NDZ	**N**on **D**etection **Z**one
ROCOF	**R**ate **O**f **C**hange **O**f **F**requency
ROCOV	**R**ate **O**f **C**hange **O**f **V**oltage
ROCOF	**R**ate **O**f **C**hange **O**f **I**mpedance
ROCOP	**R**ate **O**f **C**hange **O**f **P**ower
DG	**D**istributed **G**eneration
THD	**T**otal **H**armonic **D**istortion
SFS	**S**andia **F**requency **S**hift

Chapter 1

Introduction

Islanding is a condition in which a part of the distribution system becomes electrically isolated from the grid and still it continues to be energized by the distribution generator connected in the network. Fig 1.1 shows the part of the distribution system connected to the incoming bus of the substation. From the Fig 1.1 it can be seen that the dotted part of the distribution system was initially feed by the utility (i.e the incoming bus from the grid) and by the distributed generator connected to that part of the distribution system. If due to certain abnormalities, the dotted part of distribution system is isolated from the grid but it is still energized by the DG connected to the distribution system then that dotted portion is said to be an island comprising of load and a DG.

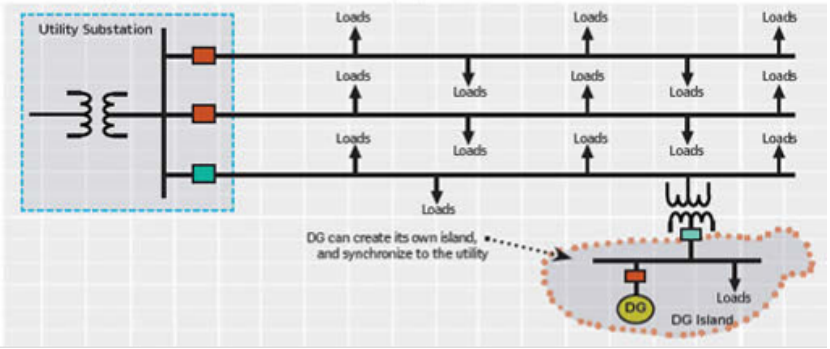

FIGURE 1.1: Distribution system connected to a substation

A DG used can be a renewable source of energy like a wind system (either a doubly fed induction generator or a permanent magnet synchronous generator) or a solar energy

system. A DG can also be based on synchronous machine with internal combustion machines, gas turbine or a hydro dams. Even though the cost of generation is more in case of energy generated using DG, DG is used in the distribution system to make up the margin between demand and the energy generated. Thereby we can improve the reliability of the system by placing the generation capacities closer to load. Also we can reduce the transmission and distribution (T&D) losses and the disturbances. Distributed Generation being connected to the distribution system at low voltage reduce the loading on transformers connected to the substation during peak hours which can improve the life of equipments connected to the substation. With the use of DG the voltage profile of the system can also be improved.

IEEE 929-1988 standard suggests the disconnection of the DG from the network once it is islanded and thereby requires all the utilities to be disconnected from the grid. Because of the mismatch between the power generated and the load that is connected to the system and also due to inadequate control of frequency and voltage, the behavior of islanded system is unpredictable.

1.1 The major issues linked with such islanded systems are:

1. **Power Quality**

   Due to the large variation of voltage and frequency the quality of power fed to the distribution system degrades in the formed island.

2. **Personnel Safety**

   Even after the removal of the grid supply from the distribution network a section of distribution system remains energized by the DG connected to the system. The line workers maintenance can sometimes prove fatal as he may be unaware of the condition.

3. **Out of Phase Recloser**

   Instantaneous reclosing can lead to out of phase reclosing which can disturb the synchronization of the DG with the grid. Sometimes there may be the case of out of phase reclosing which can lead to large currents in the system, resulting in large torques in the Rotor of synchronous generator which can permanently damage the rotor of synchronous generator.

4. **Stability Concern** Integration of DG can impact on power system voltage and frequency stability. So, it is necessary that there should not be abrupt tripping of DG.

Prolonged islanding can be extremely dangerous and can be fatal as the field personal may be unaware of the system being energized by the DG. Also, during islanding condition, voltage of the DG can go out of phase with rest of the system and reclosing the islanded system with rest of the system can lead to high currents and thus high torques in the system. Hence, there is a need for an anti-islanding algorithm that can diffrentiate the islanding events from the various non-islanding events.

1.2 Basics of Islanding detection

The basic phylosophy behind the detection of an islanding event is to monitor the DG parameters at its terminals. And the changes in the parameters can be used to differentiate the islanding event from various non-islanding events. Islanding detection techniques can be classified as one of the following as shown in the Fig 1.2.

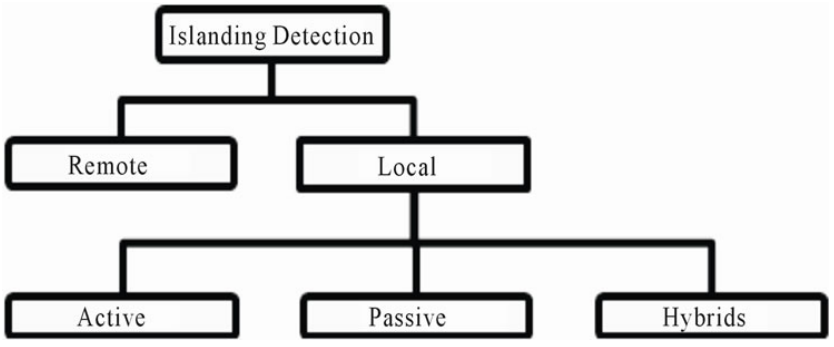

FIGURE 1.2: Distribution system connected to a substation

As shown in the figure, the islanding techniques can be broadly classified as either remote detection technique or local detection techniqes based on their working principle.

1. **Remote islanding detection techniques:**

   Remote islanding detection technique is based on the communication between the utilities and the DG's. Even though the remote detection techniques are more reliable, the remote islanding detection techniques are avoided as they are expensive.

2. **Local detection scheme**

   The local detection techniques are based on the continuous monitoring of the system parameters like voltage, frequency, current etc. These can be further classified as follows :

   (a) **Passive detection scheme**

   In passive techniques various system parameters are monitored at the DG and utilities. Some parameters monitored are voltage, frequency and power. These parameters varies greatly when the system is islanded. And the islanding events can be differentiated from the non-islanding events by the threshold set for these parameters. One of the advantages of these Passive techniques are that these are fast and they don't introduce any disturbance in the system. But the problem with this technique is that it introduces a huge non -detectable zone (NDZ), where the technique fails to differentiate the islanding events and the non-islanding events. Some of the commonly used passive detection techniques are:

   i. **Rate of change of output power:**

   The rate of change of power ($\frac{dp}{dt}$) is much more in the islanding condition than in the case when the distribution system was connected to the grid. Once the rate of change of output power is more than the set threshold value, the event is considered as an islanding event.

   ii. **Rate of change of frequency:**

   The rate of change of frequency is given by,

$$ROCOF = \frac{df}{dt} = \frac{\Delta P}{2HG} f \tag{1.1}$$

   where, ΔP is power mismatch at the DG side,

   G is the DG generation capacity,

   H is the DG moment of inertia,

   Large systems have have high value of H, G but small ones have lesser inertia and therefore the rate of change of frequency is more when there is some disturbance. The rate of change of frequency is much more in case of islanding event but it is very less in case of non-islanding event.

   iii. **Rate of change of frequency over power:**

$\frac{df}{dp}$ is large for a small system but its small for a large system. This phenomena is used to differentiate the islanding event from non-islanding events.

iv. **Voltage unbalance:**

During the islanding event, the change in the load is fed by the DG connected to the system. If the change in load is large the magnitude of voltage decreases, this change in voltage magnitude is used to detect a islanding event

v. **Harmonic distortion:**

With the change in magnitude and the configuration of load, the harmonic currents in the system changes. This change in the harmonic content is much more in case of inverter based DG. This change in the harmonic content is determined by the total harmonic distortion (THD) of the voltage. This change in THD is used to detect the islanding event.

(b) **Active detection techniques:** The problem with the passive detection technique is that it is unable detect the islanding event when the generation and the load is equal. In the active detection technique, the perturbation are introduced in the system and thus the system parameters are changed. A significant change in one of them can detect the islanding event. The problem with active detection technique is that because of the introduced perturbations voltage profile of the system may change.

(c) **Hybrid detection techniques:**

Hybrid detection technique employs both passive and active detection techniques. But the active technique is used when the passive technique is suspected.

The remote islanding detection technique is based on the communication between the utilities and the DG's.

1.3 Literature Survey

Various detection techniques such as passive, active, hybrid and remote have been reported in the literature. Islanding detection is also possible by the use of Neural Network tools. Remote detection technique comprising of the Power line carrier communication

(PLCC) and supervisory control and data acquisition (SCADA) monitoring signals at the utility and DG side and the absence of the signals can be termed as an islanding condition. Though remote detection technique is reliable, it requires high cost in the installation of transceivers and other monitoring devices.

Active techniques require constant injection of the power in the system which can degrade the power quality and is unable to detect islanding condition under certain conditions. Some of the well-known passive detection technique comprises of ROCOF, ROCOV vector shift/phase jump or voltage based methods. Problem with these techniques is that these techniques provide satisfactory results with high active power mismatch (15%) and with active power mismatch less than 15% it cannot guarantee a selective operation. Moreover, it may lead to nuisance tripping in case of capacitor switching or induction machine switching event [6]. With ROCOV, the islanding condition can be discriminated with the normal condition i.e. with high reactive power mismatch. Thus, with passive detection techniques the detection zone becomes very less.

Later on, several islanding detection techniques based on pattern recognition have been reported based on the Wavelet transform.This method requires to extract features from the three phase voltage and current samples using the wavelet transform. But it uses only six wavelet coefficients of just voltage sample which reduces the computational effort also it is not able to detect the islanding at low active and reactive power mismatch. One of the reported islanding detection technique based on wavelet singular entropy [12] was successful in detecting islanding events with high power mismatch. However, it's hardware implementation in real time is difficult. Detection techniques using phase locked loops was a successful islanding detection technique. But it fails in some non-islanding cases such as switching of capacitor and induction motor, short circuit on adjacent feeder and tripping of individual DG was not considered.

A technique based on rate of change of impedance was an effective method in discriminating the islanding and non-islanding event but this scheme is not able to distinguish between LLL-G fault on the adjacent feeder and the islanding condition [8]. A detection with Sandia frequency shift (SFS) and ROCOF was proposed which reduced the power quality deterioration and the non-detection zone was also reduced in comparison with the normally used SFS algorithm. But the techniques time of detection and NDZ largely depends on the passive technique threshold set. As the passive techniques detect the islanding events just by monitoring the system parameters, these are of lower cost and are widely used for DG's with lower power.

Of the commonly used passive detection techniques ROCOF is most frequently used as

it is a very fast in detecting abnormality. But one of the major drawback is very large NDZ. A classification technique based on decision tree was implemented in one of the papers. But the technique requires a very large set of parameters and sometimes it is unable to classify the events. Some passive techniques based on the fuzzy rule and the empirical mode decomposition have been reported and these methods known to perform very well. But these methods requires a large maturation period before being used. There are techniques which are based on the oscillation frequency estimation but these techniques employ a large window length of 350 to 500ms just for oscillation frequency estimation and therefore the detection time is very much.

To overcome the above problems a detection is developed which is based on the oscillation frequency estimation but the technique uses a very small window size. Thereby the overall detection time reduces significantly. The detection technique uses a window length of 2.5 ms and it is therefore a very fast detection method.

1.4 Objectives of Dissertation Work

The objectives of this dissertation work include:

1. Propose an islanding detection scheme based on an machine learning tool of random forest technique.
2. Propose an islanding detection scheme based on passive islanding detection scheme.
3. Developing a robust islanding detection scheme that can differentiate the islanding events from various non-islanding events even for perfect power matching condition.

1.5 Organisation of Report

This report is organized as follows:

1. Chapter 2: A novel islanding detection scheme implemented using the random forest scheme on the negative sequence voltage is given in this chapter. This chapter also gives the brief description of the classifier Random forest technique.

2. Chapter 3: A passive detection scheme based on the oscillation frequency of the synchronous generator is shown is described in this chapter. This chapter also gives the information related to the oscillation frequency of the synchronous generator.

3. Chapter 4 This is the concluding part of the thesis. This chapter also gives the information about the scope for the future work

4. Appendix

Chapter 2

Proposed Scheme: Islanding detection using Random forest technique

---

Machine learning tools can be used to differentiate one class of events from the other. In the proposed scheme machine learning tool of Random forest technique is used to classify the islanding events from the different non-islanding events based on the negative voltage samples obtained by simulating these events in RSCAD/RTDS software.

2.1 Random Forest Algorithm

Random forest technique [6] because of the distinctive feature of being consistently accurate, being highly efficient on large sets of data and for being robust for noise, is widely used in classification of the data samples in the field of image processing, the study of fault classification in power system and so on. Random forest is a collection of un-pruned regression or classification trees. Random forest generates many trees for classification, constructed using tree classification algorithm by using different bootstrap sample from the set of original data. The tree structured classifier is of the type h(x,k), where k here is independently distributed random vectors. After the formation of forest if a new object is to be classified then it is put down each tree for deciding the class for the object. Class for the object is decided on the basis of number of votes (indicating

trees decision) attained by each tree after being put down on it. Errors in generalizing depends on the individual tree strength within the forest and the correlation between them. The algorithm can be divided in two important parts namely growth of each tree and that of the voting period.

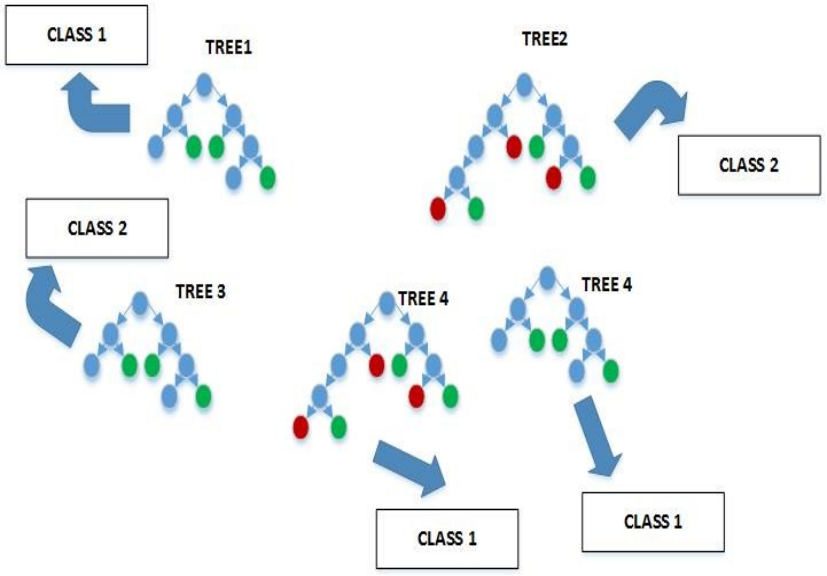

FIGURE 2.1: Decision of class of the sample on the basis of number of votes

Each sample is passed through the number of decision trees and each decision tree votes for the class of the sample. On the basis of majority of votes, the class of the sample is decided. Let h1(x), h2(x), hn(x) be the set of classifiers. Also let Y,X be a random vector sampled from the training data. The margin function is given by [3]

$$mg(X,Y) = av_k I(h_k(X) = Y) - max(av_k I(h_k(X) = J) \tag{2.1}$$

where I(*) is the indicator function. The margin measures the extent to which the average numbers of voters at X,Y for the right class exceeds than the other class. Based on this function, the generalization error is given by

$$PE^* = P_{X,Y}(mg(X,Y) < 0) \tag{2.2}$$

As the number of trees increases, for almost surely all sequences 1.PE* converge to

$$P_{X,Y}(P_\theta(h(X,\theta) = y) - maxP_\theta(h_k(X,\theta) = J) < 0 \tag{2.3}$$

An upper bound for the generalization error is given by,

$$PE^* < \rho\left(1 - \frac{S^2}{s^2}\right) \tag{2.4}$$

Although the bound is likely to be loose, it fulfills the same suggestive function for RFA as VC-type bound do for other types of classifiers. It shows that the two ingredients involved in the generalization error for RFA are the strength of individual classifiers in the forest and the correlation between them in terms of raw margin function.

2.2 Simulation Results

The block diagram of the IEEE 34 BUS system is shown in Fig.(2.2). As shown in the Fig.(2.2), multiple DGs are connected at bus 834, bus 890 and bus 840. The description of the DGs at different bus is shown in the table 1.The detailed line parameters of Bergeon line model at different nodes used in the system is given in the Appendix A.

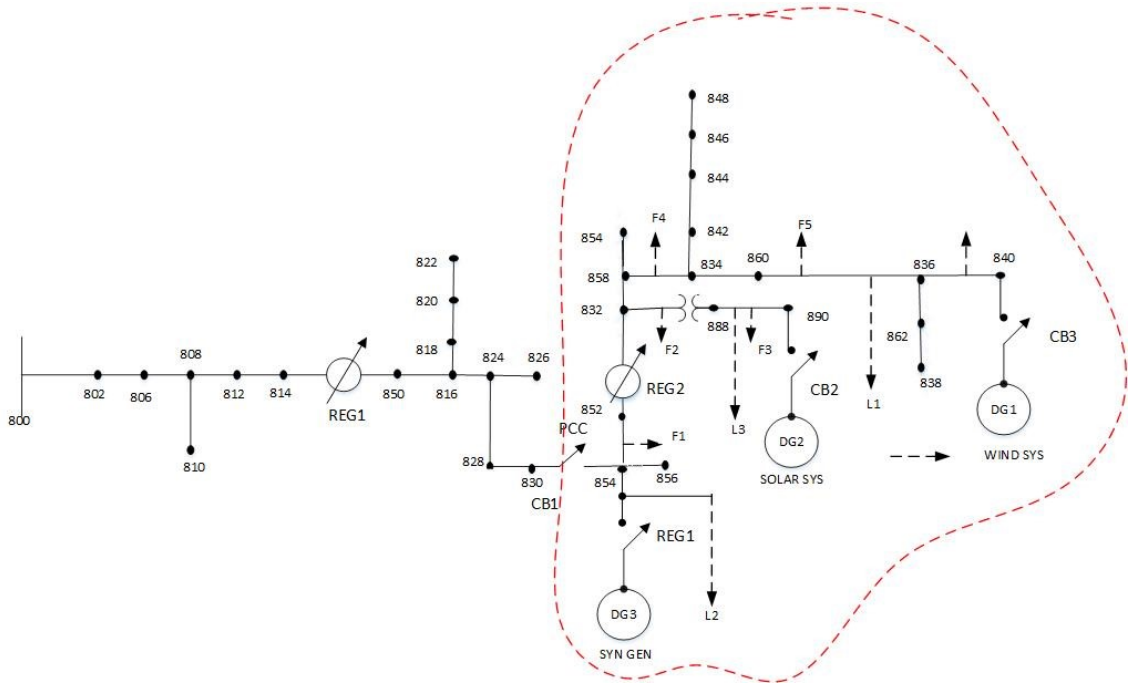

FIGURE 2.2: IEEE 34 BUS System with DG

A point of common coupling where the branches of all the DGs are connected is at bus 834. A circuit breaker connected between the bus 830 and the PCC is used to implement

TABLE 2.1: Generation capacity of different DGs at different BUS

BUS No.	DG	Rating (MVA)
834	Syn Gen	2
890	Solar	1
840	Wind	2

islanding operation. Thus after the operation of the circuit breaker the dotted part of the network becomes isolated. Transmission line parameters are used as per the standard IEEE convention defined for IEEE 34 Bus. Different simulations carried for islanding and non-islanding events are as follows:

1. ISLANDING CONDITIONS
   (a) Circuit breaker CB1 is tripped so that the dotted network is disconnected from the grid with the variation of the load.
2. NON-ISLANDING CONDITIONS
   (a) Load L1 and L2 are disconnected from the network.
   (b) Change the power factor of the load.
   (c) Switching (ON/OFF) the capacitor (C) located at bus 860 with the variation of the load.
   (d) Switching (ON/OFF) the Induction machine (IM) located at bus 860 with the variation of the load.
   (e) Short circuit faults (A-G, B-G, C-G, A-B-G, B-C-G, A-C-G, A-B-C-G) on the adjacent feeder at F1 (10% on the feeder joining the PCC and DG1), F2 (50% on the feeder joining the PCC and DG1), F3 (90% on the feeder joining the PCC and the DG1) with the variation of the load.
   (f) Tripping of other DG (DG2) from the network with the variation of the load.

2.2.1 Performance of the proposed scheme during non-islanding and islanding situation

The performance of the system for the islanding condition can be studied by the Fig 2.3 and Fig 2.4. Fig 2.3 and Fig 2.4 shows the voltage and the current profile at the

PCC respectively. From the figures it can be that there has been a dip in the 3 phase voltage magnitudes and the magnitude of the 3 phase current increases as soon as the islanding event takes place. The islanding event is said to have taken place at 0.08 secs. The reduction in the magnitude of the voltages can be attributed to the sudden increase in the load on the DG. The magnitude of voltage decrease as the sudden load is imposed on the system. Initially the power required by the load was fed by the grid and the DG's (synchronous DG, wind and solar) but as the grid is disconnected there occurs an additional burden on the DG's and thus there is a drop in the voltage levels of the system. To maintain constant power the value of current shoots up as soon as the islanding event takes place.

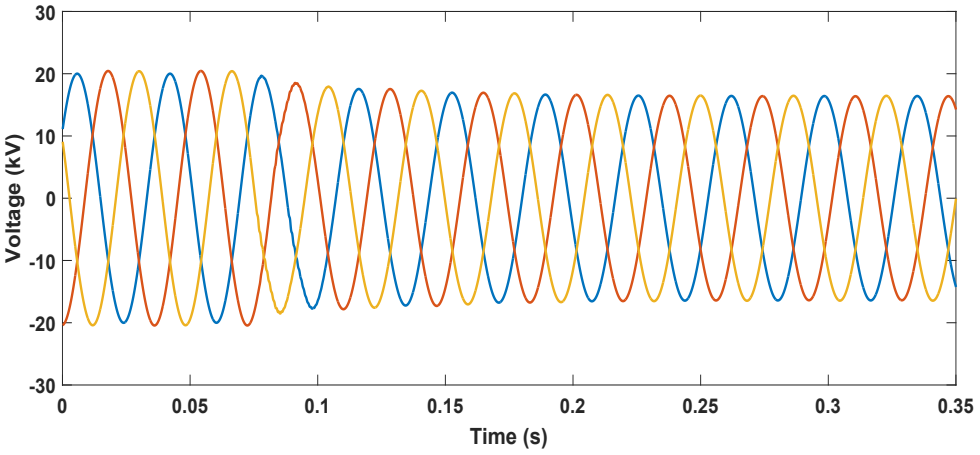

FIGURE 2.3: Change in the magnitude of 3 ph voltage for an islanding event

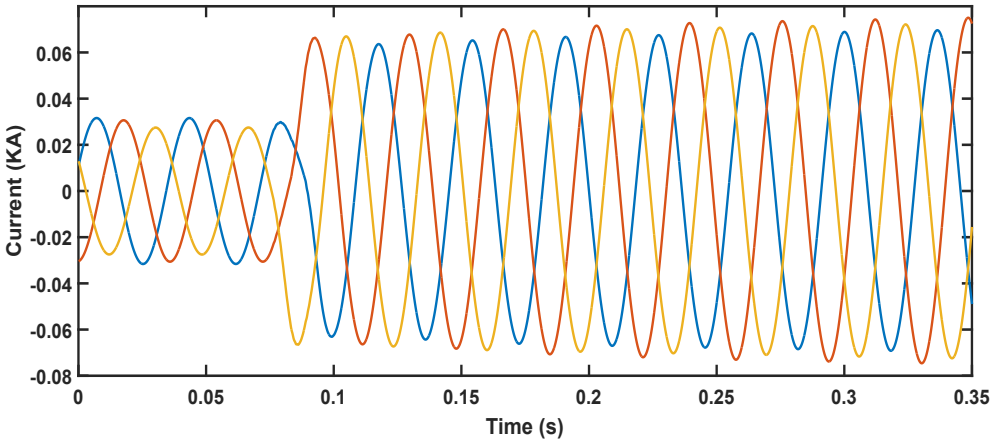

FIGURE 2.4: Change in the magnitude of 3 ph current for an islanding event

Fig. 2.3 shows the simulation result during islanding situation simulated by operation of circuit breaker (CB1) with 0% active power miss-match. The islanding situation is created at 0.04 s. Various negative sequence voltages are monitored at PCC. It has been

observed from Fig. 2.3 that the value of negative sequence voltage remains almost zero before 0.04 s whereas it increases suddenly to a high value after 0.04 s. The simulation results in terms of negative sequence voltage during non-islanding event simulated by disconnecting load L1 is shown in Fig. 2.4. It is to be noted from Fig. 2.4 that the value of negative sequence voltage remains below 0.01. Fig. 2.5 shows the simulation results for the non-islanding event of tripping of one of the DG. Here wind DG is tripped from the existing system by the operation of the circuit breaker at an instant of 0.04 sec. From Fig 2.5 it can be seen that negative sequence voltages even after the tripping of the DG, the magnitude of the negative sequence voltages remains way below 0.01 p.u. Fig 2.6 shows the negative sequence voltages

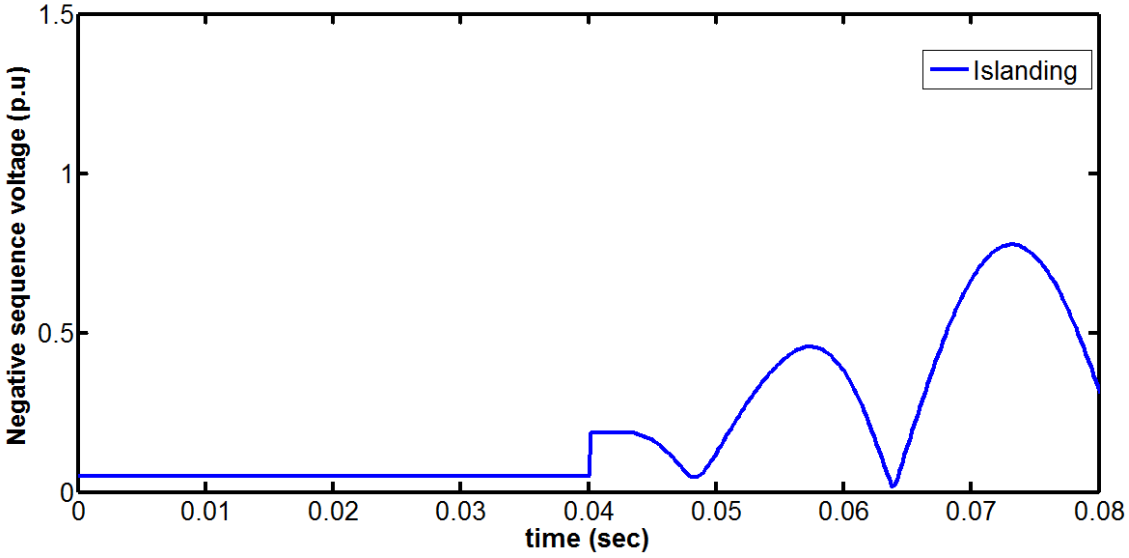

FIGURE 2.5: Negative sequence voltages during islanding situation simulated by operation of circuit breaker (CB1) with 0% active power mis-match

for switching of the capacitor in the system at Bus 834. Here in this system capacitor switching is simulated by the operation of the circuit breaker. From the Fig. 2.6 it can be seen that the introduction of capacitor in the system can create some disturbances in the magnitudes of the negative sequence voltages of the system. But the variation in the magnitude of the negative sequence voltages is less than 0.1 p.u. Fig 2.7 shows the simulation results for the $LLL-G$ fault simulated at F4 between Bus 858 and 834. From the Fig. 2.7 it can be observed that the negative sequence voltage magnitude remains below 0.04 p.u. even in case of $LLL-G$ fault. Fig 2.8 shows the negative sequence voltages for the non-islanding event of switching of the induction motor. The event of switching of induction motor is simulated by the operation of circuit breaker at Bus 834. The magnitude of negative sequence voltage again remains below 0.05 even in

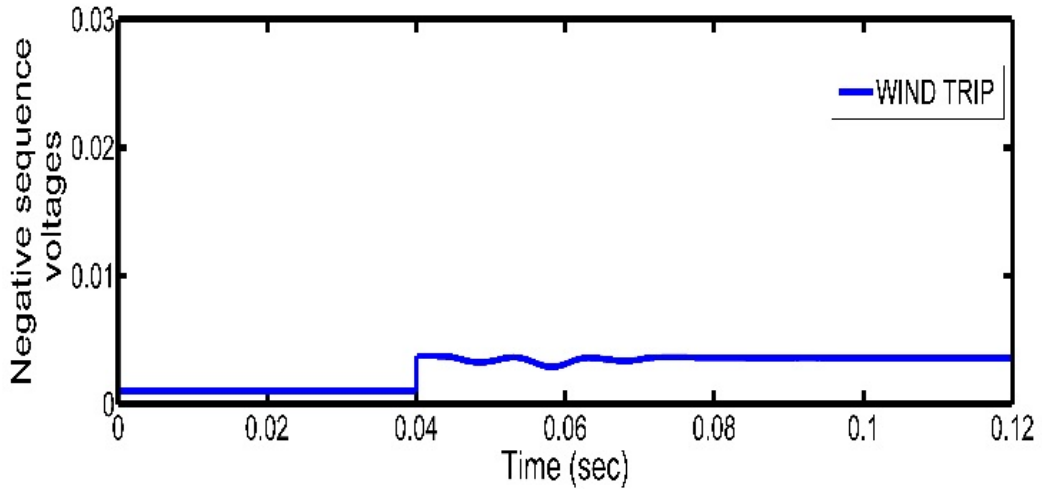

FIGURE 2.6: Negative sequence voltage during non-islanding event simulated by disconnecting load L1

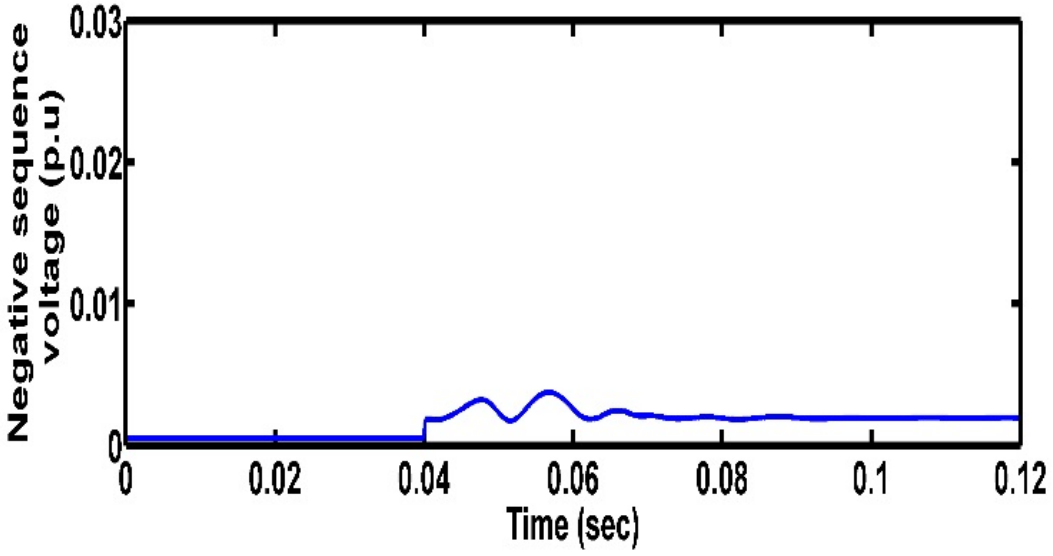

FIGURE 2.7: Negative sequence voltage during non-islanding event simulated by disconnecting one of the DG (Wind)

case of switching of the induction motor. From Fig 2.3 to Fig 2.8, it can be seen that there is a large difference in the magnitude of negative sequence voltages for islanding event and for other non-islanding events. Thus the scheme can be effectively utilized for differentiating the different islanding and non-islanding events. It is to be noted that the system remains stable during the simulation of the non-islanding events. The proposed scheme is capable in differentiating the islanding event from the $L-L-L-G$ fault where some other schemes failed.

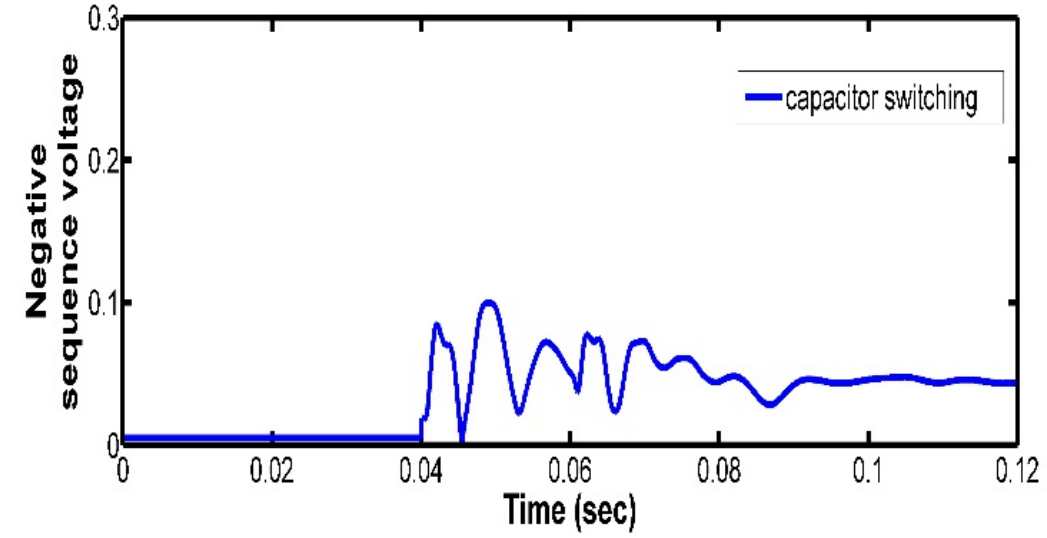

FIGURE 2.8: Negative sequence voltage during non-islanding event simulated switching (ON) of the capacitor

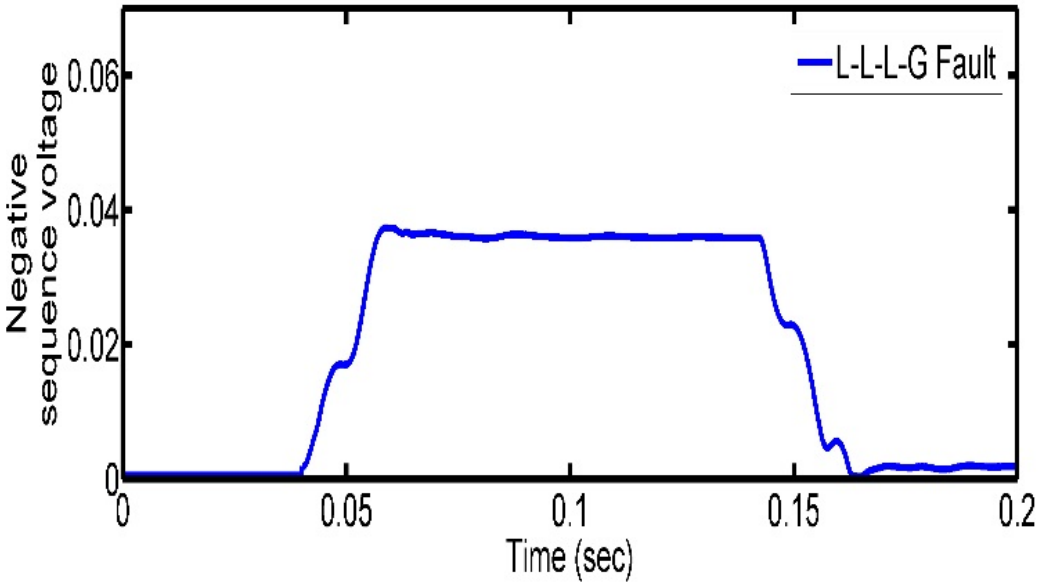

FIGURE 2.9: Negative sequence voltage during non-islanding event generated by simulating L-L-L-G fault

2.2.2 Formation of the confusion matrix and implementation of random forest technique

Fig 2.9. Shows the flowchart for the application of the Random forest technique to the different samples of negative sequence voltages obtained by simulating different islanding and non-islanding events. In the proposed scheme random forest technique is used to distinguish different islanding events from the non-islanding events. From the flowchart it can be seen that first different sequence voltages are acquired by simulating

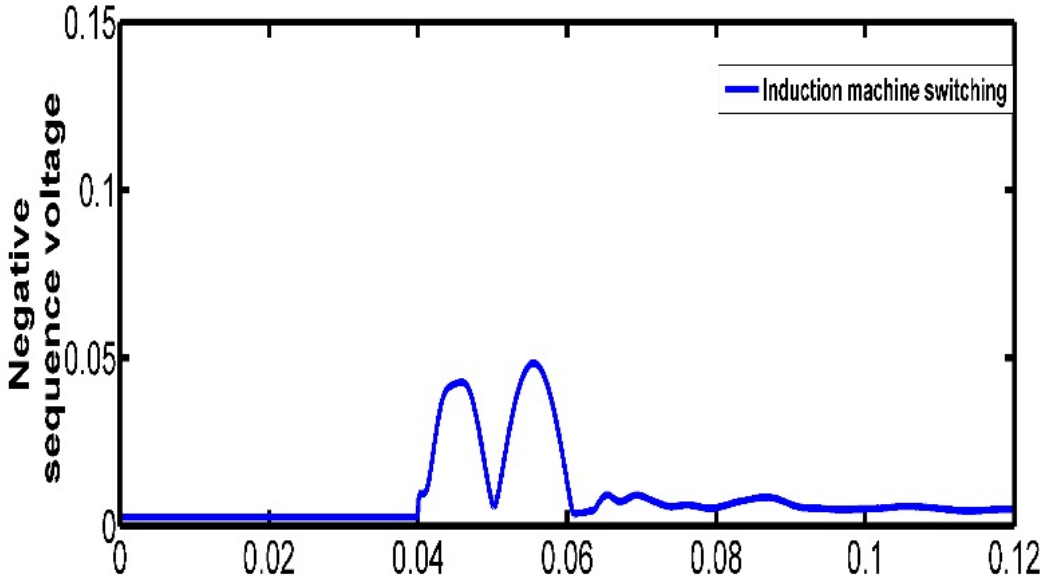

FIGURE 2.10: Negative sequence voltage during non-islanding event simulated by switching of the Induction motor

the different abnormal events by the simulating software RSCAD/RTDS. After acquiring different voltage samples, a data set is formed by compiling different negative sequence voltages forming different data class for different islanding and non-islanding samples. Now different samples each from islanding and the non-islanding events are selected for the formation of training set. With the formation of the training set, scheme is now able to predict the relation between different data sets. Now different set of test samples of different data class can be effectively classified in islanding or non-islanding set of data. For the effective classification of the data sets different parameters like ntree and the different set of training and test data plays an important role. And thus for the application of the random forest technique different combinations of ntree and different sets of training and the test data were experimented. From fig 2.10 it can be observed that the accuracy varies for different combinations of ntree. From the figure it can be observed that the accuracy of classification is maximum for ntree=200. Another experiment was conducted by varying the number of training and the test set data. Different sets of test and training data sets used are 50% training 50% testing, 60% training 40% testing, 70% training 30% testing, 80% training 20% testing. With different combination of testing and training set it has been found that the accuracy is maximum for the testing and the training combination of 60% training and 40% testing. Fig 2.10 shows the variation of classification accuracy with the number of tree (ntree).

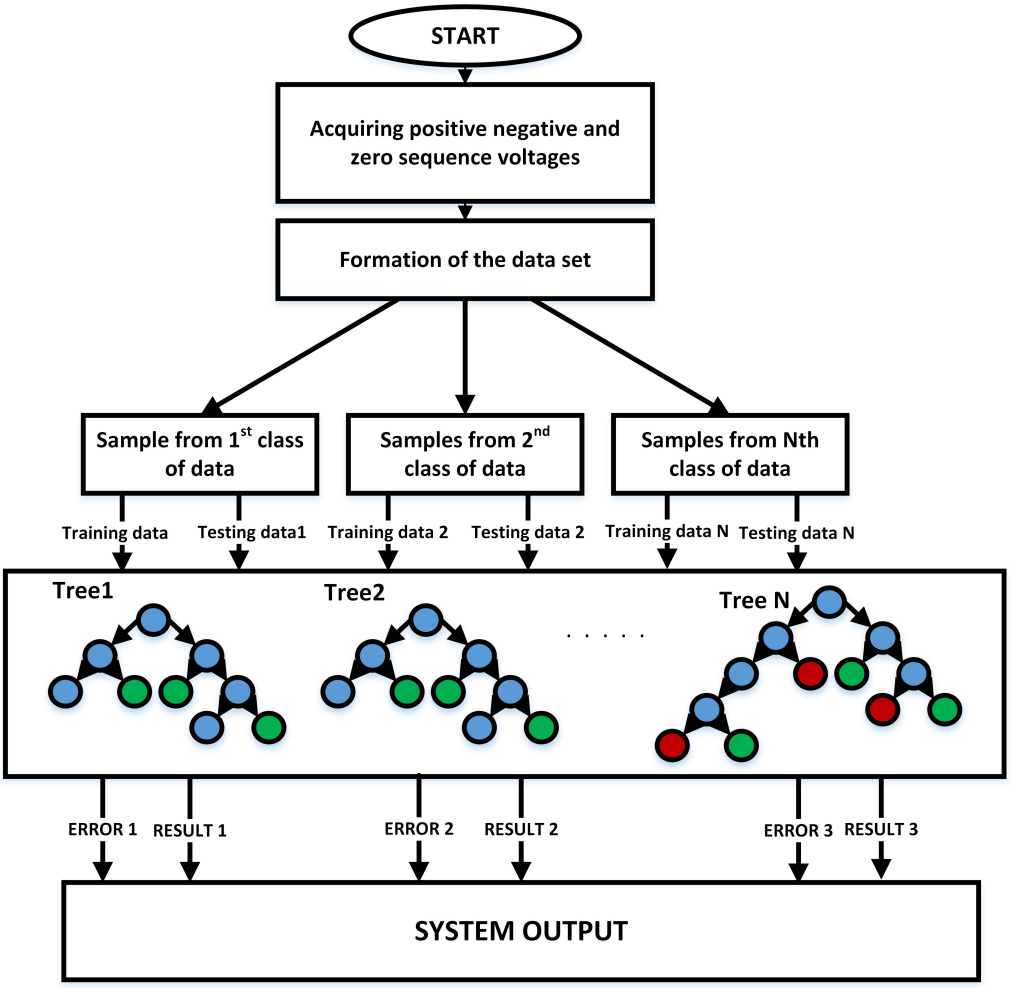

FIGURE 2.11: Flowchart for implementing the Random forest technique in the proposed scheme

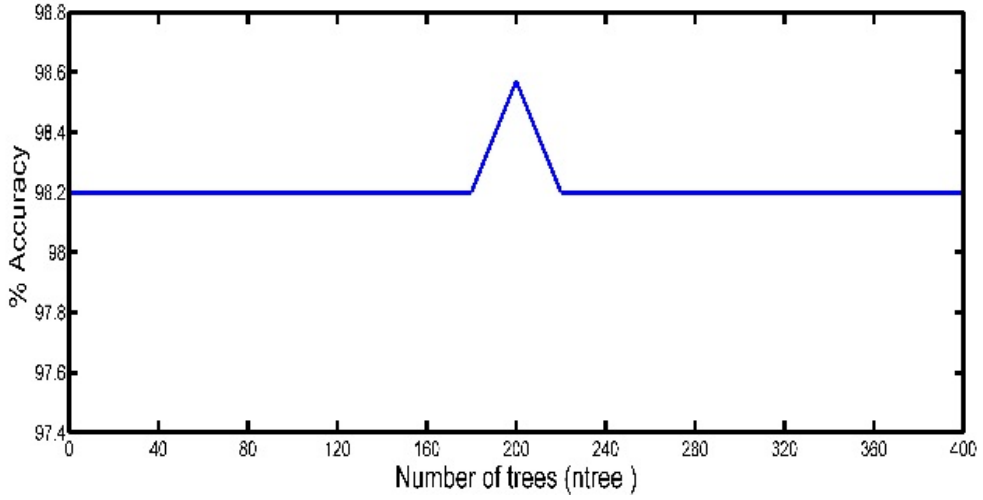

FIGURE 2.12: Negative sequence voltage during non-islanding event simulated by disconnecting load L1

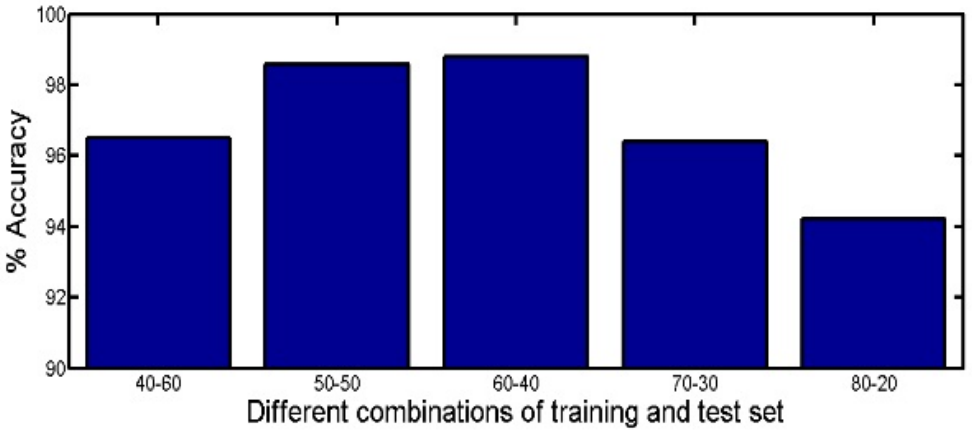

FIGURE 2.13: Variation of accuracy with different combination of test set and training set

2.3 Comparison of the results obtained from the proposed scheme with other methods

Table 2.2 shows the classification accuracy of the proposed scheme in comparison with the classification accuracy of other methods. From the table it can be seen that the classification accuracy for the proposed scheme is more than that for other methods like Nave Bayesian classifier, Support vector machine and decision tree classifier. Thus the proposed scheme is able to classify the islanding event form non-islanding event with high classification accuracy.

TABLE 2.2: Comparison of the results obtained with the already implemented techniques

Classifier	Accuracy (%)
Proposed scheme	98.81
Nave Bayesian Classifier	82
Support vector machine	94
Decision Tree	97

The results obtained for the detection of the islanding event by the application of random forest technique on the negative sequence voltages was found out to be highest around 98.81% in comparison to the accuracy of other methods as mentioned in [5].

2.4 Conclusion

A new islanding detection scheme based on Random Forest classifier has been presented in this paper. In order to evaluate the validity of the proposed scheme, large numbers of islanding/non-islanding cases have been simulated by modeling IEEE 34-bus system in RTDS software. It is to be noted from the simulated results that the proposed scheme is able to detect islanding event accurately and rapidly.

Chapter 3

Proposed Scheme: Island detection of distributed generation based on the frequency of oscillation

---

This technique aims in detecting the islanding event based on the frequency of oscillation of angle between the Stator and the Rotor. The frequency of oscillation is different for the islanding and non-islanding events and this property is used to differentiate the islanding events from various non-islanding events.

3.1 Basics related to Oscillation frequency of the synchronous Generator

For synchronous machine the angle between the stator and the rotor remains almost constant for the steady state conditions. But during some abnormal events such as when there is a large change in the load (i.e change between the generation capacity and the load applied) or when there occurs some short circuit fault phenomenon in the system, angle between the stator and rotor adjust itself to provide the required magnetic

field. This change in the angle between stator and rotor leads to the oscillation of stator and the rotor and it is given by the differential equation given by

$$\frac{2H}{w_0}\frac{d^2\delta}{dt^2} + \frac{Dd\delta}{dt} = P_m - P_e \tag{3.1}$$

where δ is the stator angle with respect to that of the rotor, t is the time in sec, H is the inertia constant of the generator, D is the damping coefficient, w_0 is the synchronous speed of the generator, P_m is the input fed to the generator and P_e is the electrical power output of the DG.

The electrical power input to the synchronous generator

$$P_e = P_m sin\delta \tag{3.2}$$

A small perturbation in $\Delta\delta$ from the initial operating position δ_0 can be represented by

$$\delta = \delta_0 + \Delta\delta \tag{3.3}$$

Due to small perturbation the swing can be linearized as given below

$$\frac{2H}{W_0}\frac{d^2\Delta\delta}{dt^2} + \frac{Dd\Delta\delta}{dt} + P_s\Delta\delta = 0 \tag{3.4}$$

where P_s is known as the synchronizing power coefficient and is defined by equation 3.5

$$P_s = P_m cos\delta_0 \tag{3.5}$$

solving the differential eqn 3.1 we get, the deviation of the frequency is given by

$$\Delta w = \frac{\Delta\delta}{dt} = -\frac{w_0\Delta\delta(0)}{\sqrt{1-\zeta^2}}e^{-\zeta w_n t}sinw_d t \tag{3.6}$$

where

$$w_d = w_n\sqrt{1-\zeta^2} \tag{3.7}$$

$$\zeta = \frac{D}{2}\sqrt{\frac{w_0}{2HP_s}} \tag{3.8}$$

$$w_n = \sqrt{\frac{w_0}{2H}P_s} \tag{3.9}$$

3.2 Frequency variation during the islanding events

During an islanding event due the absence of supply from the main system, the synchronizing coefficient is zero. Thus, the equation

$$\frac{2H}{w_0}\frac{d^2\Delta\delta}{dt^2} + \frac{Dd\Delta\delta}{dt} = \Delta P \tag{3.10}$$

where Δ P is the variation in power due to islanding event. In other words, Δ P the eletrical power transmitted at the split point. It is assumed the Δ P ramains constant during the islanding event. If the power flows from the DG to the split point Δ P is positive. The rotor angle being synchronized with the stator magnetic feild before the islanding event takes place, following initial conditions are considered for equation 3.10, $\Delta\delta(0) = 0$ and $d\Delta\delta(0)/dt = 0$

The solution of the above equation is given in terms of the change in the electrical frequency and it is as shown below,

$$\Delta w = \frac{d\Delta\delta}{dt} = \frac{\Delta P}{D}(1 - e^{(-w_0 D/2H)t)} \tag{3.11}$$

Comparing equations 3.6 to 3.11 it can be concluded that the frequency varies differently during the islanding and during the normal events. During the normal operating conditions the frequency oscillates with the damped natural frequency of w_d. But during islanding events the frequency does not oscillate but it is given by an exponential response.

3.3 Frequency Estimation

The synchronous generators oscillate at a very low frequency and it is in the range of few Hertz. The frequency of oscillation estimation method proposed can be derived as follows:

Let the deviation of the frequency from the rated value is given by equation 3.4.

$$\Delta w_k = w_k - w_0 \tag{3.12}$$

where w_0 is the rated frequency of the system and w_k is the electrical frequency at the k^{th} instant.The frequency deviation from equation 3.6 with damping effect neglected can be written in discretized and simplified way as

$$\Delta w_k = Acos\left(w_{osc}k\Delta t - \frac{\pi}{2}\right) \tag{3.13}$$

where A is the amplitude of oscillation and w_{osc} is the frequency of oscillation. Considering the other two delay from N and 2N

$$\Delta w_{k-N} = Acos(w_{osc}(k-N)\Delta t - \frac{\pi}{2}) \tag{3.14}$$

$$\Delta w_{k-N} = Acos(w_{osc}(k-2N)\Delta t - \frac{\pi}{2}) \tag{3.15}$$

Addition equations (3.13), (3.14) and dividing by (3.15) we get,

$$\frac{\Delta w_k + \Delta w_{k-2N}}{\Delta w_{k-N}} = \frac{cos(w_{osc}(k)\Delta t - \frac{\pi}{2}) + cos(w_{osc}(k-2N)\Delta t - \frac{\pi}{2})}{cos(w_{osc}(k-N)\Delta t - \frac{\pi}{2})} \tag{3.16}$$

The solution of the above equation 3.16 is given by

$$w_{osc}(k) = \frac{1}{2N\Delta t} acos(\frac{w_k + w_{k-2N} - 2w_0}{w_{k-N} - w_0}) \tag{3.17}$$

In Hertz the equation can be written as in equation 3.18

$$f_osc(k) = \frac{f_sample}{2\pi N} acos(\frac{f(k) + f(k-2N) - 2f_0}{2f(k-N) - 2f_0}) \tag{3.18}$$

where f_{sample} is the sampling frequency, acos is the arc cosine, f(k) is the oscillation frequency ar a particular instant k, and N is the half of the window size. While simulating the sampling frequency was set as 2000 samples in a total duration of runtime of 0.5 sec. Therefore one cycle of the frequency curve has 80 samples and thus the value of N is selected to be 10. Smaller the value of N ensures the faster working of the algorithm but it degrades the accuracy of the algorithm. The arc cosine function returns the real values in the range of [0,π]. As the frequency signal is not pure cosine function during some islanding situations, (f(k)+ f(k-2N)-2 f_0) may be greater than (2f(k-N)-2f_0). In these cases the function value may cross the limits of [-1,1] and thus for these cases the value of arc cosine is taken to be zero. But this does not effect the performance of the algorithm as this algorithm was verified during islanding and by setting the oscillation frequency to zero which makes islanding detection possible.

3.4 Simulation Results

3.4.1 Performance of the system parameters during the Islanding condition

Fig 3.1 shows the changes in the 3 phase voltage profile when the islanding event takes place. Initially, the load in the distribution part was fed by the grid and also by the DG's connected. With the operation of the circuit breaker to disconnect the dotted part of the system as shown in Fig 3.3 from the grid, the load in that part of the system has to be fed by the DG only so there is sudden change in the load on DG. Thus there is a sudden dip in the voltage levels which can be observed in the Fig 3.1. Now the load has to fed with the defined power but as the voltage decreases, the magnitude of current has to be increased to meet up the requirements. Fig 3.2 shows the current profile during islanding operation. We can see that there is an increase in the current levels.

Fig 3.3 shows the system that was simulated in $RSCAD/RTDS$. Different islanding and non-islanding events are simulated on the system. From figure it can be seen that different DG's are placed at bus 610 and bus 64. DG's placed are synchronous generator and wind energy system of $3MVA$ and $1MVA$ respectively. The transmission line

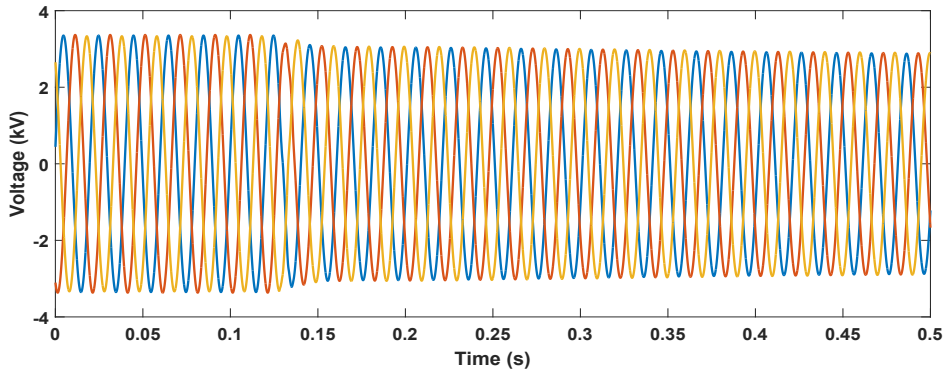

FIGURE 3.1: Changes in the voltage profile during Islanding

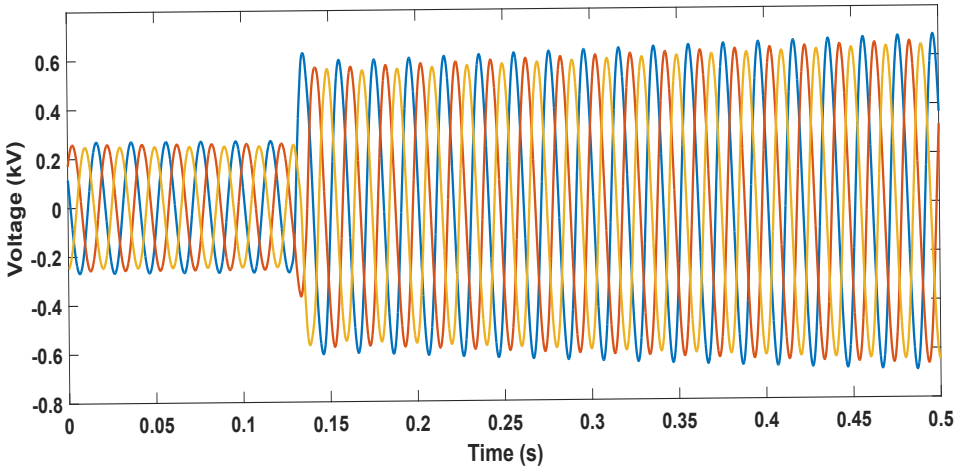

FIGURE 3.2: Changes in the current profile during Islanding

parameters for lines between different buses. bus 60 is the point which is connected to the branches connected to both the DG's. Base load of $0.2MW$ with the power factor of 0.92 is connected at bus 64 along with the loads connected at different nodes of the distribution system as per the standard IEEE 123 Bus system. Variation of frequency is monitored at bus 60 for different islanding and non-islanding events.

Different simulations that were tried for Islanding and non-islanding events are as follows:

1. **Islanding conditions**

   (a) Operation of the circuit breaker (CB) between bus 13 and 152, CB connected between bus 94 and bus 54 CB at bus 60.

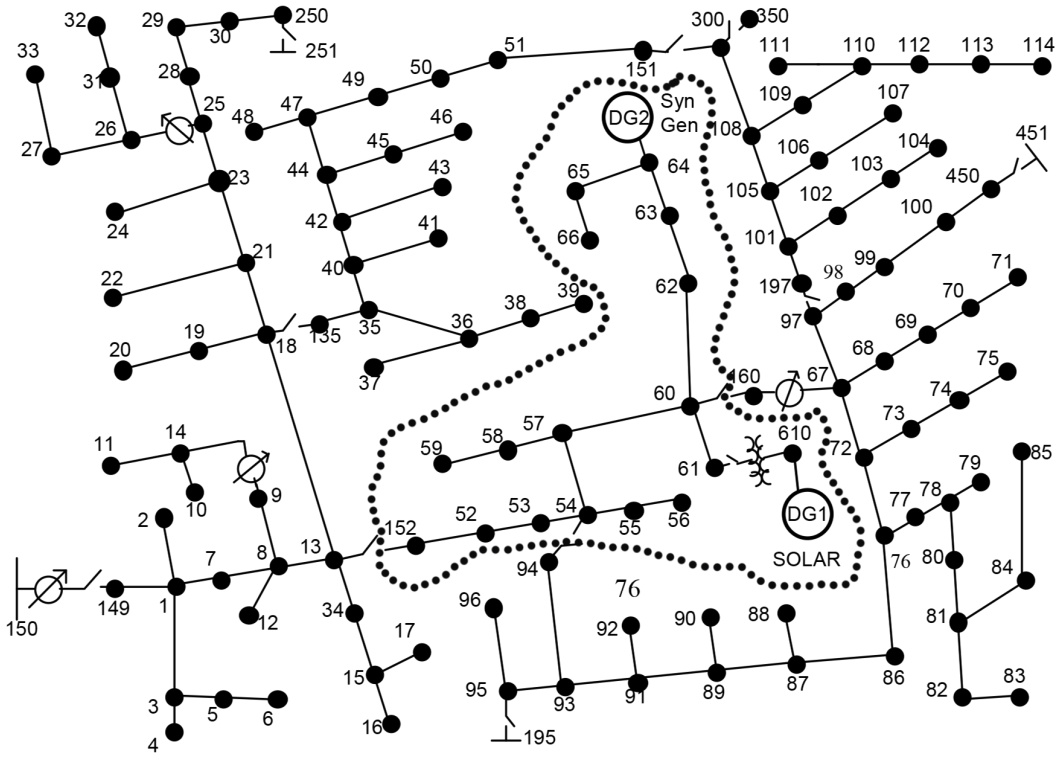

FIGURE 3.3: IEEE 123 BUS System with DG

2. **Non-Islanding conditions**

   (a) Load at BUS 64 is disconnected by the operation of the circuit breaker

   (b) Change the power factor of the load.

   (c) Switching (ON/OFF) the capacitor (C) located at bus 860 with the variation of load.

   (d) Switching (ON/OFF) the Induction machine (IM) located at bus 860 with the variation of the load

   (e) Short circuit faults (A-G, B-G, C-G, A-B-G, B-C-G, AC-G,A-B-C-G) on F1(10 % on the feeder joining the PCC and DG1),F2 (50 % on the feeder joining PCC and DG1), F3 (90 % on the feeder joining PCC and the DG1) with the variation of the load at adjacent feeder.

   (f) Tripping of other DG (Solar DG) from the network with the variation of the load.

Normally the variation in frequency is in the range of 20-50mHz. But for the abnormal condition there may be some variation of frequency more than 50mHz. The variation

of frequency for different events is monitored at bus 64. Fig 3.4 shows the variation of frequency curve for the islanding event. From the figure it can be seen that the value of frequency varies up to $50.6Hz$. The variation of frequency for load switching is shown in Fig 3.5. From the figure it can be seen that the frequency can sometime rise about $10mHz$. Similarly for the event of switching of capacitor from Fig 3.6 it can be seen that frequency may remain in the range of $10mHz$. For Fig 3.7 which is the plot for the variation of frequency for induction machine it can be seen that the frequency dips to $49.94Hz$ initially and then it tries to catch up normal base frequency of $50Hz$. For the variation of frequency for the DG tripping it can be seen that the frequency increases up to $50.018Hz$ as shown in the Fig 3.8 . Thus for the following cases the frequency may change more than $20mHz$. Thus the threshold may be set to $20mHz$.

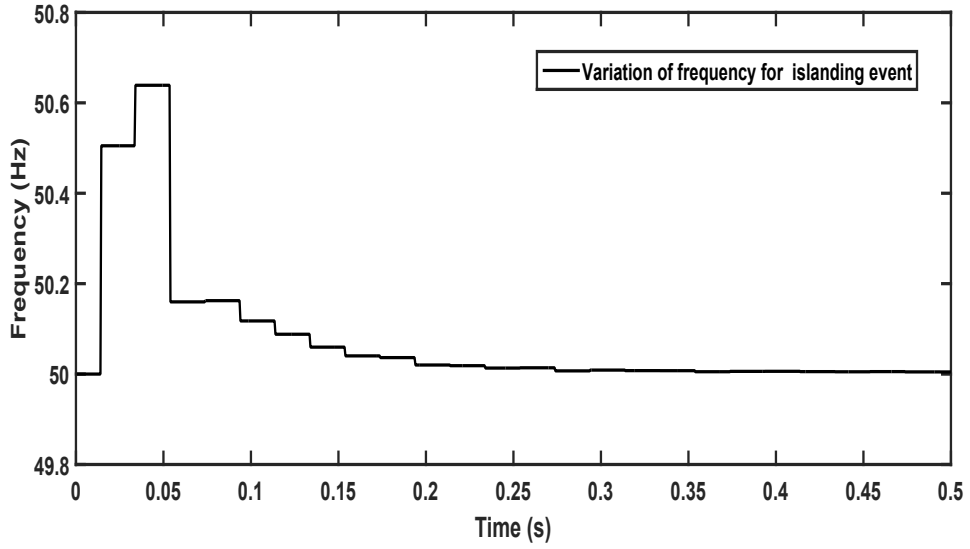

FIGURE 3.4: Variation of frequency for Islanding conditions

3.5 Proposed Algorithm

Fig 3.9 shows the algorithm for the islanding detection based on the oscillation frequency of the generator. From the algorithm it can be seen that frequency monitored at the terminal of the DG is first compared to the set threshold value. In the previous article it was shown that during the abnormal condition the frequency varies more than $20mHz$. Thus in the proposed algorithm the value of threshold was set to $20mHz$. When the variation of frequency exceeds the threshold value i.e $|f - 60| > Th1$ the oscillation

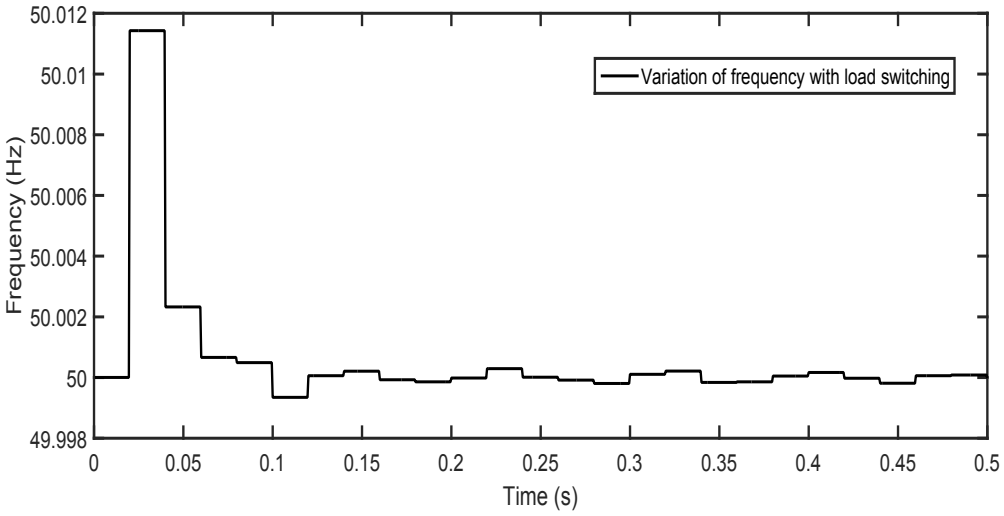

FIGURE 3.5: Variation of frequency for Load switching conditions

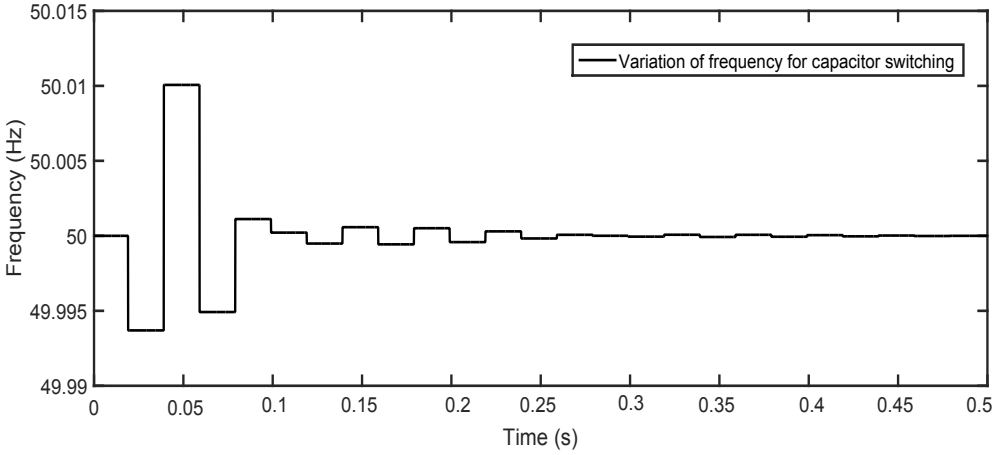

FIGURE 3.6: Variation of frequency for an event of capacitor switching

frequency is calculated which was described in the section 3.3. The oscillation frequency is calculated as per the following equation

$$f_osc(k) = \frac{f_sample}{2\pi N} acos(\frac{f(k) + f(k-2N) - 2f_0}{2f(k-N) - 2f_0}) \tag{3.19}$$

Thus the oscillation frequency is calculated for the abnormal conditions i.e various islanding and non-islanding events. Fig 3.10 to Fig 3.15 shows the plot of oscillation frequency for different islanding and non-islanding events. Fig 3.10 shows the plot for oscillation frequency of the synchronous generator. From the plot it can be seen that as

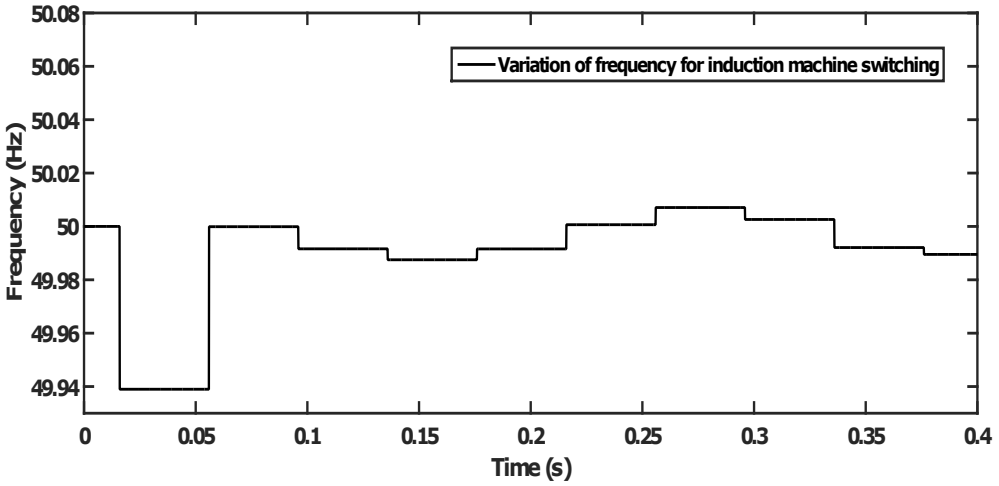

FIGURE 3.7: Variation of frequency for an event of induction machine switching

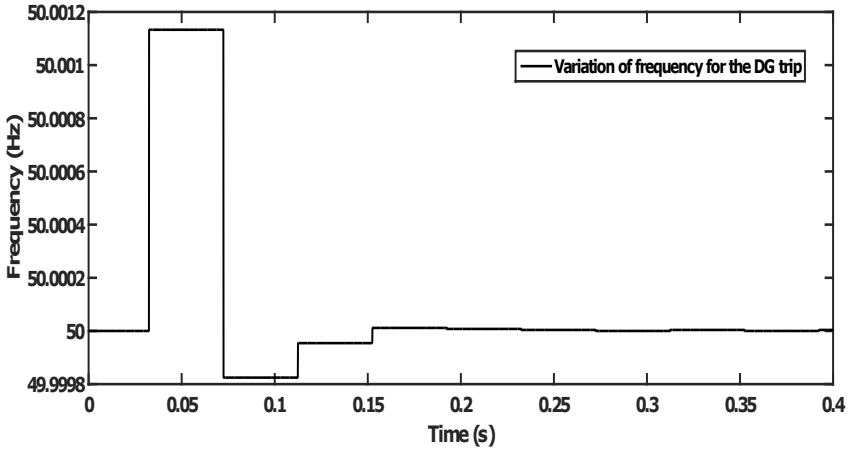

FIGURE 3.8: Variation of frequency for an event of DG tripping

soon as the islanding event took place, the value of the oscillation frequency decreases exponentially (value of magnitude of peaks) as the time passes by. It can also be observed that the magnitude of peak after 2^{nd} and 3^{rd} peak remains below the $2.5Hz$ and thus the value of threshold Th_2 can be set as $2.5Hz$. And the number of times the peak crosses $2.5Hz$ is two. Thus the threshold Th3 can be set as 3 (To improve the robustness of the system). Fig 3.11 shows the variation of the oscillation frequency for load switching. From the figure it can be shown that multiple times the value of peak remains greater than $2.5Hz$. Now, as the value crosses threshold of three (No of times the peak crosses threshold value). Fig 3.12 shows the variation of oscillation frequency for the capacitor

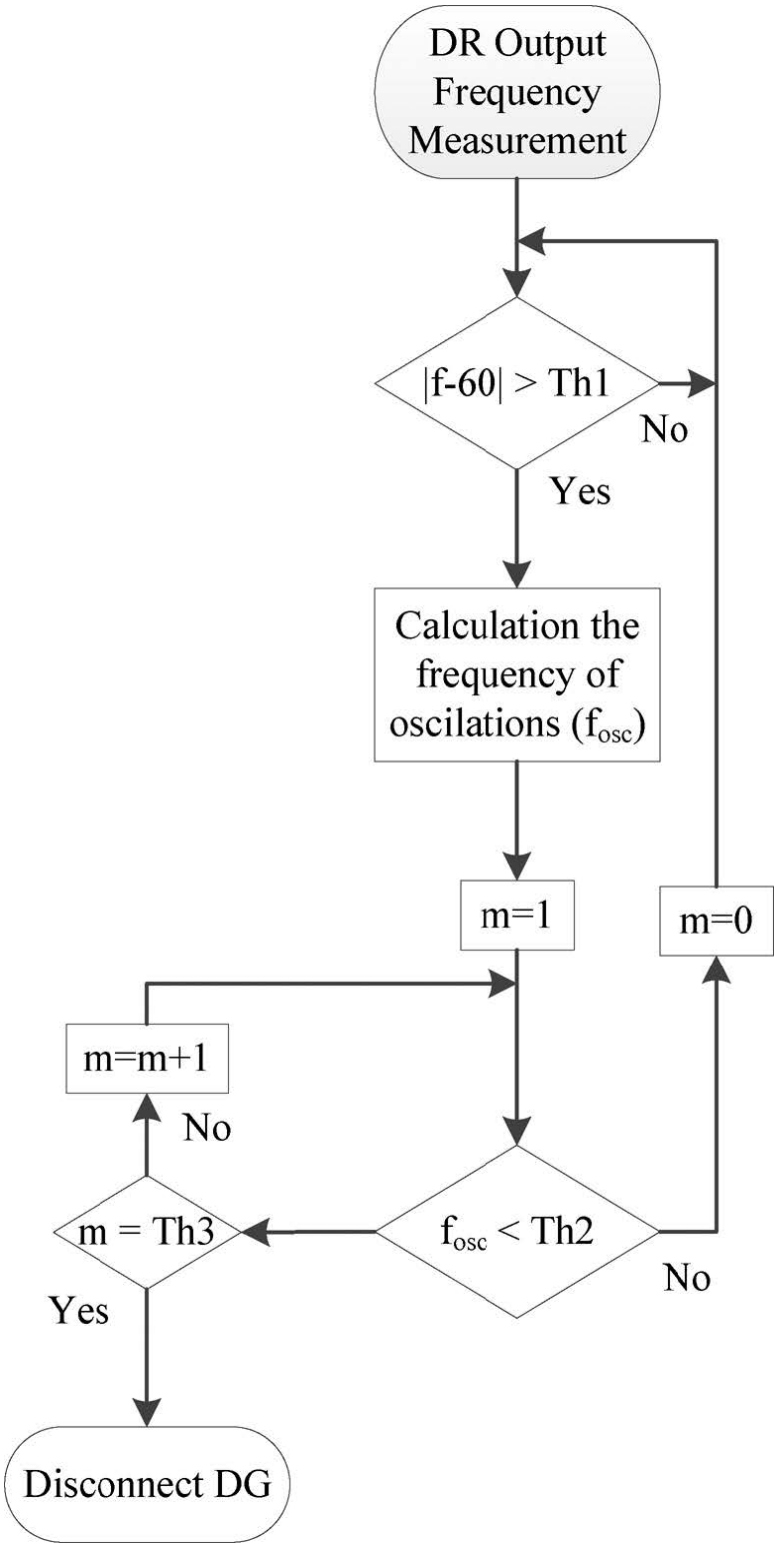

FIGURE 3.9: Algorithm for Islanding detection

switching. From the figure it can be seen that again multiple times the peak value exceeds the threshold of Th_2 and Th_3. Thus as the threshold (Th_3) value increases beyond

the set value and the event can be considered as an non-islanding event. Plot for Oscillation frequency for LLL-G fault event is shown in Fig 3.13. Even for LLL-G fault the oscillation frequency plot has multiple peaks which crosses the Threshold value of Th_2. Similarly we can differentiate the islanding event from the non-islanding event of DG tripping. Even for DG tripping with the multiple peaks crossing the threshold multiple times (more than 3). Thus, the different non-islanding events can be differentiated from the non-islanding events by following the proposed algorithm. The proposed algorithm is tested for different values of base load at bus and with different values of generation levels of DG. And it was found that the proposed scheme is capable in detecting the islanding events.

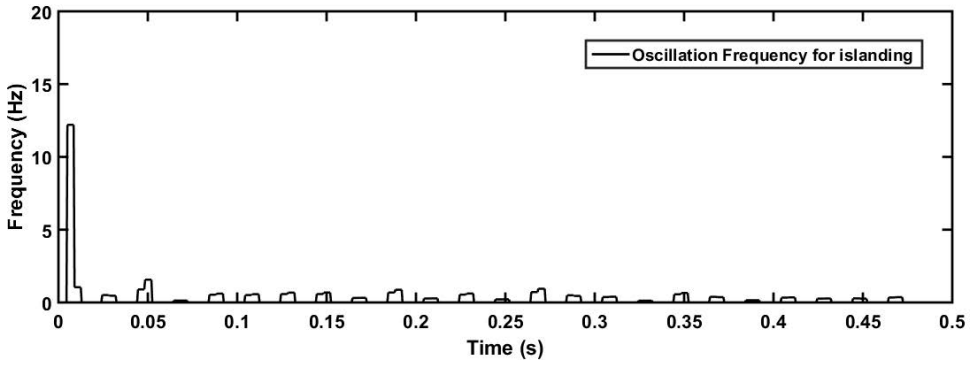

FIGURE 3.10: Oscillation frequency for Islanding conditions

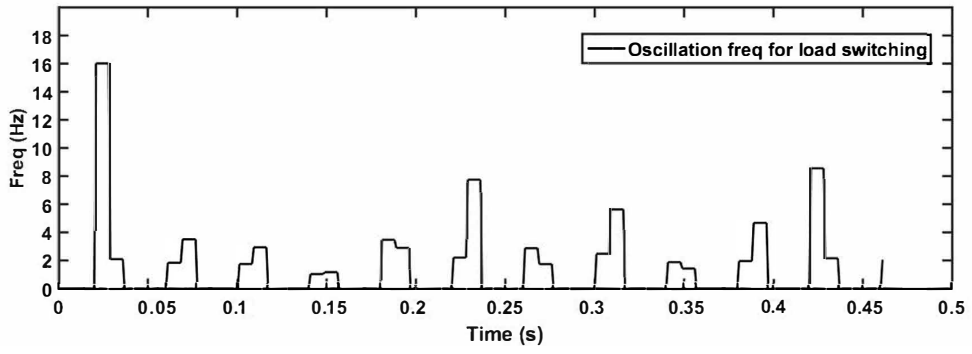

FIGURE 3.11: Oscillation frequency for an event of Load switching

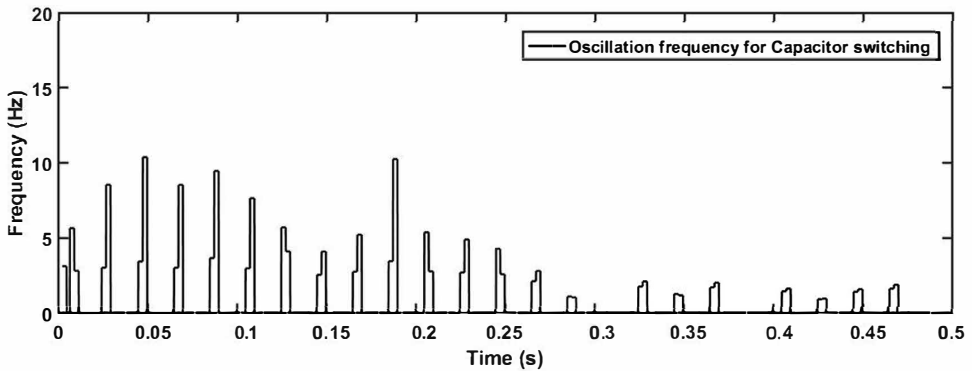

FIGURE 3.12: Oscillation frequency for an event of Capacitor switching

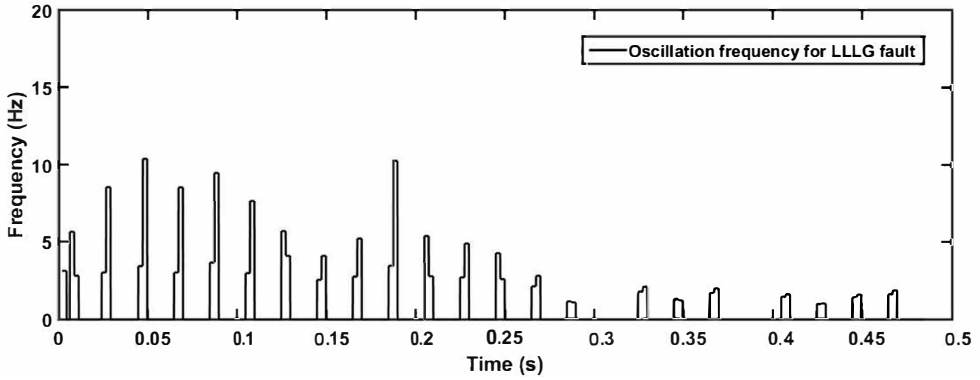

FIGURE 3.13: Oscillation frequency for a LLL-G fault

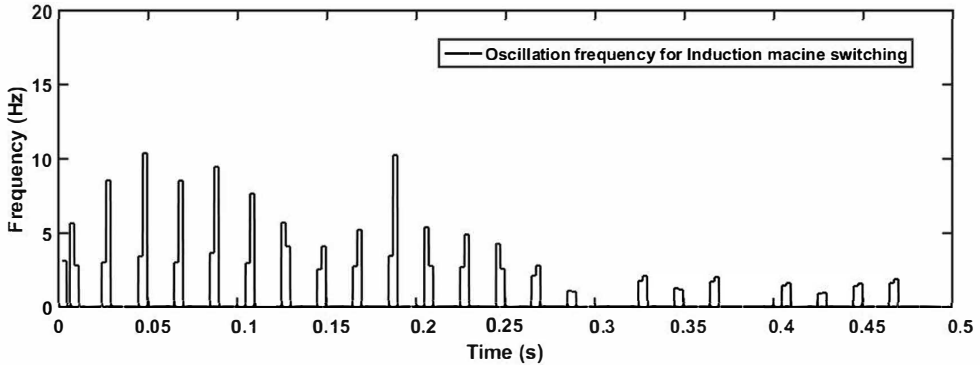

FIGURE 3.14: Oscillation frequency for an event of switching of induction machine

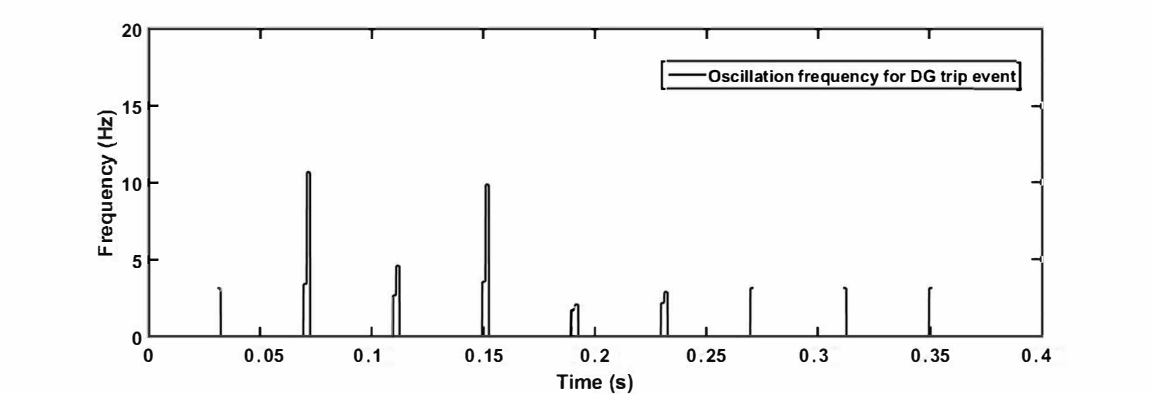

FIGURE 3.15: Oscillation frequency for tripping of solar generator

3.6 Performance of the technique for different values of load and the mismatch

The performance of the technique is tested for different values of the load and the mismatch with the generation capacity. Table 3.1 shows the performance of the technique for different values of the load. Generation capacity of the system during the islanded condition is 3.65MW.

TABLE 3.1: Performance of the scheme for different values of Power mismatch

Load (MW)	**% Mismatch**	**Maloperation of technique**
3.2	12	NO
3.3	9.5	NO
3.4	6.84	NO
3.45	5.47	YES
3.5	4.10	YES
3.55	2.74	YES
3.6	1.30	YES
3.65	0	YES
3.7	-1.3	YES
3.75	-2.74	YES
3.8	-4.10	YES
3.85	-5.47	YES
3.95	-6.84	NO
4.05	-9.5	NO
4.15	-12	NO

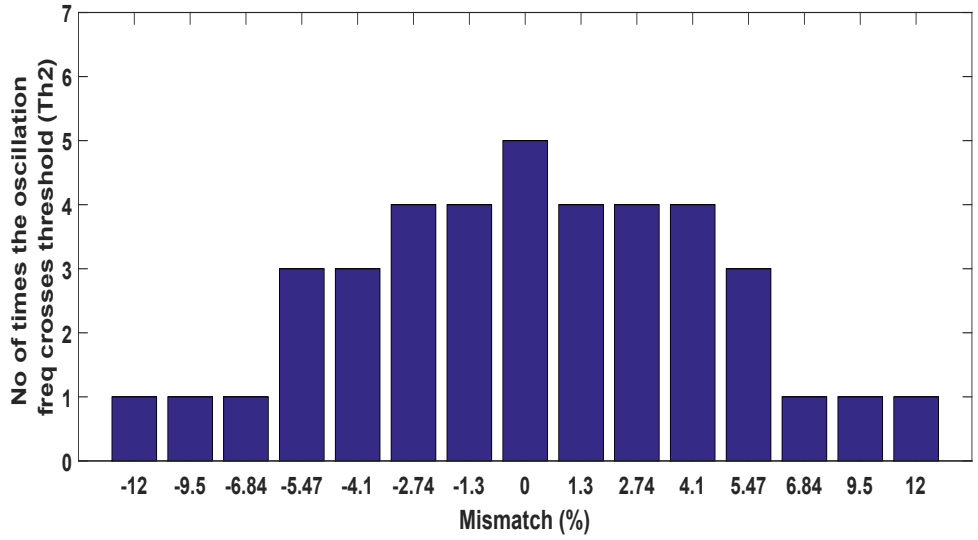

FIGURE 3.16: Performance of the scheme for different power mismatch

It has been found that the technique maloperates for the mismatch of or less than 5.47% where the load is greater than 3.45MW and less than 3.85MW. Fig 3.16 shows the bar chart showing the number of times the oscillation frequency curve crosses the threshold (Th_2).From the fig 3.16 it can be seen that with % mismatch of -12% to -5.47% the oscillation frequency crosses the threshold for just one time and therefore it successfully detects the abnormality as an islanding event. But when islanding occurs for a mismatch of less than 5.47% the number of times it crosses the threshold value is three which is more than the set threshold value and therefore it is not successful in detecting the islanding event in case of perfect power matching condition. This phenomenon of maloperation of the technique for mismatch between the generation capacity and the load applied is valid for both positive and negative mismatch i.e. the scheme fails for the positive values of mismatch when generation capacity is more than the load (upto $+5.47\%$) and also for the negative values of the mismatch when the load applied on the system is greater than the generation (upto -5.47%).

3.7 Conclusion

An efficient and effective passive islanding technique is proposed. This technique is based on synchronous generator oscillation frequency. The technique detects the frequency of oscillation for synchronous generator in a very less time as it uses a window length of just $2.5ms$ as compared to the window length of 350 to $500ms$ of other detection techniques.

The detection technique is a robust one as it is capable in detecting an islanding event even for very less power mismatch (5%). The technique is tested for a number of other simulation cases comprising of different islanding and non-islanding cases of different loads.

Chapter 4

Conclusion and Scope for Future Work

4.1 Conclusion

This describes two islanding detection techniques. One of them was based on the machine learning tool of Random forest technique and the other technique was based on the oscillation frequency of the synchronous generator. The schemes have been tested by simulating a large number of islanding and non-islanding cases on IEEE 34 bus and IEEE 123 bus. With the analysis of the scheme on the large system (123 bus system) the validity of the scheme on large distribution system is justified. The schemes are effective and efficient in detecting islanding event. The method involving the oscillation frequency requires a very small window length for estimating the oscillation frequency and therefore the time taken is very less in detecting an islanding event. Both the techniques are highly robust and are capable detecting even if the power mismatch is very less.

4.2 Scope for Future Work

1. A modelling of the islanding system is to be done and the techniques are to be tested for real time implementation in the field which was tested for the outputs

of RTDS.

2. The practicality of the system has to be evaluated considering the field test data and hardware aspects.

3. As 123 bus system is already modelled, the performance of the system for bigger system can be analysed easily for some other schemes already listed in the literature.

Chapter 5

Appendix

Table 5.1: Distributed load at different nodes

Node A	Node B	Load Type	Ph1 (kW)	Ph1 (kVAR)	Ph2 (kW)	Ph2 (kVAR)	Ph3 (kW)	Ph3 (kVAR)
802	806	Y-PQ	0	0	30	15	25	14
808	810	Y-I	0	0	16	8	0	0
818	820	Y-Z	34	17	0	0	0	0
820	822	Y-PQ	135	70	0	0	0	0
816	824	D-I	0	0	5	2	0	0
824	826	Y-I	0	0	40	20	0	0
824	828	Y-PQ	0	0	0	0	4	2
828	830	Y-PQ	7	3	0	0	0	0
854	856	Y-PQ	0	0	4	2	0	0
832	858	D-Z	7	3	2	1	6	3
858	864	Y-PQ	2	1	0	0	0	0
858	834	D-PQ	4	2	15	8	13	7
834	860	D-Z	16	8	20	10	110	55
860	836	D-PQ	30	15	10	6	42	22
836	840	D-I	18	9	22	11	0	0
862	838	Y-PQ	0	0	28	14	0	0
842	844	Y-PQ	9	5	0	0	0	0
844	846	Y-PQ	0	0	25	12	20	11
846	848	Y-PQ	0	0	23	11	0	0

TABLE 5.2: Transmission line parameters for different configuration

Node A	Node B	Length(ft.)	Config.
800	802	2580	300
802	806	1730	300
806	808	32230	300
808	810	5804	303
808	812	37500	300
812	814	29730	300
814	850	10	301
816	818	1710	302
816	824	10210	301
818	820	48150	302
820	822	13740	302
824	826	3030	303
824	828	840	301
828	830	20440	301
830	854	520	301
832	858	4900	301
832	888	0	XFM-1
834	860	2020	301
834	842	280	301
836	840	860	301
836	862	280	301
842	844	1350	301
844	846	3640	301
846	848	530	301
850	816	310	301
852	832	10	301
854	856	23330	303
854	852	36830	301
858	864	1620	302
858	834	5830	301
860	836	2680	301
862	838	4860	304
888	890	10560	300

TABLE 5.3: Spot load at different nodes

Node A	Load Type	Ph1 (kW)	Ph1 (kVAR)	Ph2 (kW)	Ph2 (kVAR)	Ph3 (kW)	Ph3 (kVAR)
860	Y-PQ	20	16	20	16	20	16
840	Y-I	9	7	9	7	9	7
844	Y-Z	135	105	135	105	135	105
848	D-PQ	20	16	20	16	20	16
890	D-I	150	75	150	75	150	75
830	D-Z	10	5	10	5	25	10

5.1 Appendix B

Different configuration of transmission line has different values of inductance and capacitance to find out the transmission line parameters is as given below:

1. **Configuration 1**

   Z (R +jX) in ohms per mile

$$\begin{pmatrix} 0.4576 + 1.0780j & 0.1560 + 0.5017j & 0.1535 + 0.3849j \\ & 0.4666 + 1.0482j & 0.1580 + 0.4236j \\ & & 0.4615 + 1.0651j \end{pmatrix}$$

   B in micro Siemens per mile

$$\begin{pmatrix} 5.6765 & -1.8319 & -0.6982 \\ & 5.9809 & -1.1645 \\ & & 5.3971 \end{pmatrix}$$

2. **Configuration 2**

   Z (R +jX) in ohms per mile

$$\begin{pmatrix} 0.4666 + 1.0482j & 0.1580 + 0.4236j & 0.1560 + 0.5017j \\ & 0.4615 + 1.0651j & 0.1535 + 0.3849j \\ & & 0.4576 + 1.0780j \end{pmatrix}$$

   B in micro Siemens per mile

$$\begin{pmatrix} 5.6765 & -1.8319 & -0.6982 \\ & 5.9809 & -1.1645 \\ & & 5.3971 \end{pmatrix}$$

3. **Configuration 3**

   Z (R +jX) in ohms per mile

$$\begin{pmatrix} 0.4615 + 1.0651j & 0.1535 + 0.3849j & 0.1580 + 0.4236j \\ & 0.4576 + 1.0780j & 0.1560 + 0.5017j \\ & & 0.4666 + 1.0482j \end{pmatrix}$$

   B in micro Siemens per mile

$$\begin{pmatrix} 5.6765 & -1.8319 & -0.6982 \\ & 5.9809 & -1.1645 \\ & & 5.3971 \end{pmatrix}$$

4. **Configuration 4**

   Z (R +jX) in ohms per mile

$$\begin{pmatrix} 0.4615 + 1.0651j & 0.1535 + 0.3849j & 0.1580 + 0.4236j \\ & 0.4576 + 1.0780j & 0.1560 + 0.5017j \\ & & 0.4666 + 1.0482j \end{pmatrix}$$

   B in micro Siemens per mile

$$\begin{pmatrix} 5.3971 & -1.1645 & -0.6982 \\ & 5.9809 & -1.8319 \\ & & 5.6765 \end{pmatrix}$$

5. **Configuration 5**

   Z (R +jX) in ohms per mile

$$\begin{pmatrix} 0.4666 + 1.0482j & 0.1560 + 0.5017j & 0.1580 + 0.4236j \\ & 0.4576 + 1.0780j & 0.1535 + 0.3849j \\ & & 0.4615 + 1.0651j \end{pmatrix}$$

   B in micro Siemens per mile

$$\begin{pmatrix} 5.9809 & -1.8319 & -1.1645 \\ & 5.6765 & -0.6982 \\ & & 5.3971 \end{pmatrix}$$

6. **Configuration 6**

   Z (R +jX) in ohms per mile

$$\begin{pmatrix} 0.4576 + 1.0780j & 0.1535 + 0.3849j & 0.1560 + 0.5017j \\ & 0.4615 + 1.0651j & 0.1580 + 0.4236j \\ & & 0.4666 + 1.0482j \end{pmatrix}$$

   B in micro Siemens per mile

$$\begin{pmatrix} 5.9809 & -1.8319 & -1.1645 \\ & 5.3971 & -1.1645 \\ & & 5.9809 \end{pmatrix}$$

7. **Configuration 7**

   Z (R +jX) in ohms per mile

$$\begin{pmatrix} 0.4576 + 1.0780j & 0.0000 & 0.1535 + 0.3849j \\ 0.0000 & 0.0000 & 0.0000 \\ & & 0.4615 + 1.0651j \end{pmatrix}$$

   B in micro Siemens per mile

$$\begin{pmatrix} 5.1154 & 0.0000 & -1.0549 \\ & 0.0000 & 0.0000 \\ & & 5.1704 \end{pmatrix}$$

8. **Configuration 8**

   Z (R +jX) in ohms per mile

$$\begin{pmatrix} 0.4576 + 1.0780j & 0.1535 + 0.3849j & 0.0000 \\ & 1.0651 & 0.0000 \\ & & 0.000 \end{pmatrix}$$

   B in micro Siemens per mile

$$\begin{pmatrix} 5.1154 & -1.0549 & 0.0000 \\ & 5.1704 & 0.0000 \\ & & 0.000 \end{pmatrix}$$

9. **Configuration 9**

   Z (R +jX) in ohms per mile

$$\begin{pmatrix} 1.3292 + 1.3475j & 0.0000 & 0.0000 \\ & 0.0000 & 0.0000 \\ & & 0.000 \end{pmatrix}$$

   B in micro Siemens per mile

$$\begin{pmatrix} 4.5193 & 0.000 & 0.0000 \\ & 5.1704 & 0.0000 \\ & & 0.000 \end{pmatrix}$$

10. **Configuration 10**

    Z (R +jX) in ohms per mile

$$\begin{pmatrix} 0 & 0.0000 & 0.0000 \\ & 0.0000 & 0.0000 \\ & & 1.3292 + 1.3475j \end{pmatrix}$$

    B in micro Siemens per mile

$$\begin{pmatrix} 0.000 & 0.000 & 0.000 \\ & 0.000 & 0.0000 \\ & & 4.5193 \end{pmatrix}$$

11. **Configuration 11**

    Z (R +jX) in ohms per mile

$$\begin{pmatrix} 0 & 0.0000 & 0.0000 \\ & 0.0000 & 0.0000 \\ & & 1.3292 + 1.3475j \end{pmatrix}$$

    B in micro Siemens per mile

$$\begin{pmatrix} 0.000 & 0.000 & 0.000 \\ & 4.5193 & 0.0000 \\ & & 0.000 \end{pmatrix}$$

12. **Configuration 12**

Z (R +jX) in ohms per mile

$$\begin{pmatrix} 1.5209 + 0.7521j & 0.5198 + 0.2775j & 0.4924 + 0.2157j \\ & 1.5329 + 0.7162j & 0.5198 + 0.2775j \\ & & 1.5209 + 0.7521j \end{pmatrix}$$

B in micro Siemens per mile

$$\begin{pmatrix} 67.2242 & 0.0000 & 0.0000 \\ & 67.2242 & 0.0000 \\ & & 67.2242 \end{pmatrix}$$

TABLE 5.4: Transmission line parameters for different configuration

Node A	Node B	Length(ft.)	Config.
1	2	175	10
1	3	250	11
1	7	300	1
3	4	200	11
3	5	325	11
5	6	250	11
7	8	200	1
8	12	225	10
8	9	225	9
8	13	300	1
9	14	425	9
13	34	150	11
13	18	825	2
14	11	250	9
14	10	250	9
15	16	375	11
15	17	350	11
18	19	250	9
18	21	300	2
19	20	325	9
21	22	525	10
21	23	250	2
23	24	550	11
23	25	275	2
25	26	350	7
25	28	200	2
26	27	275	7
26	31	225	11
27	33	500	9
28	29	300	2
29	30	350	2
30	250	200	2
31	32	300	11
34	15	100	11
35	36	650	8
35	40	250	1
36	37	300	9
36	38	250	10
38	39	325	10

TABLE 5.5: Transmission line parameters for different configuration (cont.)

Node A	Node B	Length(ft.)	Config.
40	41	325	11
40	42	250	1
42	43	500	10
42	44	200	1
44	45	200	9
44	47	250	1
45	46	300	9
47	48	150	4
47	49	250	4
49	50	250	4
50	51	250	4
51	151	500	4
52	53	200	1
53	54	125	1
54	55	275	1
54	57	350	3
55	56	275	1
57	58	250	10
57	60	750	3
58	59	250	10
60	61	550	5
60	62	250	12
62	63	175	12
63	64	350	12
64	65	425	12
65	66	325	12
67	68	200	9
67	72	275	3
67	97	250	3
68	69	275	9
69	70	325	9
70	71	275	9
72	73	275	11
72	76	200	3
73	74	350	11
74	75	400	11
76	77	400	6
76	86	700	3
77	78	100	6

TABLE 5.6: Transmission line parameters for different configuration (cont.)

Node A	Node B	Length(ft.)	Config.
78	79	225	6
78	80	475	6
80	81	475	6
81	82	250	6
81	84	675	11
82	83	250	6
84	85	475	11
86	87	450	6
87	88	175	9
87	89	275	6
89	90	225	10
89	91	225	6
91	92	300	11
91	93	225	6
93	94	275	9
93	95	300	6
95	96	200	10
97	98	275	3
98	99	550	3
99	100	300	3
100	450	800	3
101	102	225	11
101	105	275	3
102	103	325	11
103	104	700	11
105	106	225	10
105	108	325	3
106	107	575	10
108	109	450	9
108	300	1000	3
109	110	300	9
110	111	575	9
110	112	125	9
112	113	525	9
113	114	325	9
135	35	375	4
149	1	400	1
152	52	400	1
160	67	350	6

Table 5.7: Transmission line parameters for different configuration (cont.)

Node A	Node B	Length(ft.)	Config.
197	101	250	3
84	85	475	11
86	87	450	6
87	88	175	9
87	89	275	6
89	90	225	10
89	91	225	6
91	92	300	11
91	93	225	6
93	94	275	9
93	95	300	6
95	96	200	10
97	98	275	3
98	99	550	3
99	100	300	3
100	450	800	3
101	102	225	11
101	105	275	3
102	103	325	11
103	104	700	11
105	106	225	10
105	108	325	3
106	107	575	10
108	109	450	9
108	300	1000	3
109	110	300	9
110	111	575	9
110	112	125	9
112	113	525	9
113	114	325	9
135	35	375	4
149	1	400	1
152	52	400	1
160	67	350	6
197	101	250	3

Table 5.8: Distributed load at different nodes

Node	Load Type	Ph1 (kW)	Ph1 (kVAR)	Ph2 (kW)	Ph2 (kVAR)	Ph3 (kW)	Ph3 (kVAR)
1	Y-PQ	40	20	0	0	0	0
2	Y-PQ	0	0	20	10	0	0
4	Y-PR	0	0	0	0	40	20
5	Y-I	0	0	0	0	20	10
6	Y-Z	0	0	0	0	40	20
7	Y-PQ	20	10	0	0	0	0
9	Y-PQ	40	20	0	0	0	0
10	Y-I	20	10	0	0	0	0
11	Y-Z	40	20	0	0	0	0
12	Y-PQ	0	0	20	10	0	0
16	Y-PQ	0	0	0	0	40	20
17	Y-PQ	0	0	0	0	20	10
19	Y-PQ	40	20	0	0	0	0
20	Y-I	40	20	0	0	0	0
22	Y-Z	0	0	40	20	0	0
24	Y-PQ	0	0	0	0	40	20
28	Y-I	40	20	0	0	0	0
29	Y-Z	40	20	0	0	0	0
30	Y-PQ	0	0	0	0	40	20
31	Y-PQ	0	0	0	0	20	10
32	Y-PQ	0	0	0	0	20	10
33	Y-I	40	20	0	0	0	0
34	Y-Z	0	0	0	0	40	20
35	D-PQ	40	20	0	0	0	0
37	Y-Z	40	20	0	0	0	0
38	Y-I	0	0	20	10	0	0
39	Y-PQ	0	0	20	10	0	0
41	Y-PQ	0	0	0	0	20	10
42	Y-PQ	20	10	0	0	0	0
43	Y-Z	0	0	40	20	0	0
45	Y-I	20	10	0	0	0	0
46	Y-PQ	20	10	0	0	0	0
47	Y-I	35	25	35	25	35	25
48	Y-Z	70	50	70	50	70	50
49	Y-PQ	35	25	70	50	35	20
50	Y-PQ	0	0	0	0	40	20
51	Y-PQ	20	10	0	0	0	0
52	Y-PQ	40	20	0	0	0	0
53	Y-PQ	40	20	0	0	0	0

TABLE 5.9: Distributed load at different nodes (cont.)

Node	Load Type	Ph1 (kW)	Ph1 (kVAR)	Ph2 (kW)	Ph2 (kVAR)	Ph3 (kW)	Ph3 (kVAR)
55	Y-Z	20	10	0	0	0	0
56	Y-PQ	0	0	20	10	0	0
58	Y-I	0	0	20	10	0	0
59	Y-PQ	0	0	20	10	0	0
60	Y-PQ	20	10	0	0	0	0
62	Y-Z	0	0	0	0	40	20
63	Y-PQ	40	20	0	0	0	0
64	Y-I	0	0	75	35	0	0
65	D-Z	35	25	35	25	70	50
66	Y-PQ	0	0	0	0	75	35
68	Y-PQ	20	10	0	0	0	0
69	Y-PQ	40	20	0	0	0	0
70	Y-PQ	20	10	0	0	0	0
71	Y-PQ	40	20	0	0	0	0
73	Y-PQ	0	0	0	0	40	20
74	Y-Z	0	0	0	0	40	20
75	Y-PQ	0	0	0	0	40	20
76	D-I	105	80	70	50	70	50
77	Y-PQ	0	0	40	20	0	0
79	Y-Z	40	20	0	0	0	0
80	Y-PQ	0	0	40	20	0	0
82	Y-PQ	40	20	0	0	0	0
83	Y-PQ	0	0	0	0	20	10
84	Y-PQ	0	0	0	0	20	10
85	Y-PQ	0	0	0	0	40	20
86	Y-PQ	0	0	20	10	0	0
87	Y-PQ	0	0	40	20	0	0
88	Y-PQ	40	20	0	0	0	0
90	Y-I	0	0	40	20	0	0
92	Y-PQ	0	0	0	0	40	20
94	Y-PQ	40	20	0	0	0	0
95	Y-PQ	0	0	20	10	0	0
96	Y-PQ	0	0	20	10	0	0
98	Y-PQ	40	20	0	0	0	0
99	Y-PQ	0	0	40	20	0	0
100	Y-Z	0	0	0	0	40	20
102	Y-PQ	0	0	0	0	20	10

Table 5.10: Distributed load at different nodes (cont.)

Node	Load Type	Ph1 (kW)	Ph1 (kVAR)	Ph2 (kW)	Ph2 (kVAR)	Ph3 (kW)	Ph3 (kVAR)
103	Y-PQ	0	0	0	0	40	20
104	Y-PQ	0	0	0	0	40	20
106	Y-PQ	0	0	40	20	0	0
107	Y-PQ	0	0	40	20	0	0
109	Y-PQ	40	20	0	0	0	0
111	Y-PQ	20	10	0	0	0	0
112	Y-I	20	10	0	0	0	0
113	Y-Z	40	20	0	0	0	0
114	Y-PQ	20	10	0	0	0	0

Bibliography

[1] A. Samui and S. Samantray, "Wavelet Singular Entropy based islanding detection in distributed generation," *IEEE Transactions on Power Delivery,* vol. 28, no. 1, pp. 411-418, Jan 2013.

[2] D. Richard, "IEEE Standard for Interconnecting Distributed Resources in to Electric Power Systems," *IEEE Standard,* pp. 1547-1549, July 2003.

[3] J.-D. Yan and Ren-Wu, "Fault Diagnosis of Power Electronic Circuit Based on Random Forests Algorithm," *IEEE International Conference on Natural Computation,.*

[4] w. Freitas, w. xu, C. Affonso and Z. Huang, "Comparative Analysis Between ROCOF and Vector Surge Relays for Distributed Generation Applications," *IEEE Transactions on Power Delivery,*vol. 20, no. 2, pp. 1315-1324, April 2005.

[5] O. N. Faqhruldin, E.-S. Ehab F and H. Hatem, "A Universal Islanding Detection Technique for Distributed Generation Using Pattern Recognition," *IEEE TRANSACTIONS ON SMART GRID,*vol. 5, no. 4, pp. 1985-1989, JULY 2014.

[6] O. N. Faqhruldin, E. F. El-Saadany and H. H. Zeineldin, "A Universal Islanding Detection Technique for Distributed Generation Using Pattern Recognition," *Electrical Power and Components,* Electrical Power and Components, vol. 40, no. 10, pp. 1149-1159, 2012.

[7] M. Garmrudi, H. Nafisi, A. Fereidouni and Hashemi, "A Novel Hybrid Islanding Detection Technique Using Rate of Voltage Change and Capacitor Tap Switching," *IEEE Trans. Instrum. Meas.,* vol. IM-35, no. 4, pp. 640-642, Dec. 1986.

[8] P. Shah and B. Bhalja, "A New Rate of Change of Impedance-based Islanding Detection Scheme in Presence of Distributed Generation," *Electric Power Components and Systems,* vol. 42, no. 7, pp. 1172-1180, July 2014.

[9] S. Natarajan, "Electric Power Components and Systems," *IEEE Trans. Instrum. Meas.,* vol. 38, no. 6, pp. 1083-1087, Dec. 1989.

[10] B. Bhalja and K. Sareen, "A New Islanding Detection Technique for Distribution System during DG Interconnections," *IEEE-Innovative Smart Grid technologies, Lougborough, 2015.*

[11] Y. Liu, S. Chen, M. Nakayama, and K. Watanabe, "A Hybrid Network Intrusion Detection Technique Using Random Forests,," *IEEE-Innovative Smart Grid technologies, Lougborough, 2015.*

[12] J. Z. Zulkernine and Mohammad, "Advanced grid synchronization for power converters under unbalanced and distorted conditions," *Availability, Reliability and Security (ARES06),* pp. 5173-5178, Nov. 2006.

[13] W. H. Kersting, "Radial distribution test feeders," *Transactions on Power Systems,*vol. 6, no. 3, pp. 975-985, 2001.

[14] A. Samui and S. Samantaray, "Wavelet Singular Entropy-Based Islanding Detection in Distributed Generation," *IEEE transactions on power delivery,* vol. 28, no. 1, pp. 411-418, 2013.

[15] Gustavo Marchesan, Matias Rossato Muraro, Ghendy Cardoso,Jr., Lenois Mariotto, and A. P. de Morais "Passive method for Distributed Generation Island detection based on oscillation frequency," *IEEE Transaction on power delivery,* vol. 31, no. 1, pp. 1355-1367, Mar. 2016.

[16] D. Velasco, C. Trujillo, G. Garcera, and E. Figueres, "An active anti-islanding method based on phase-PLL perturbation," *IEEE Trans. Power Electron,* vol. 26, no. 4, pp. 10561066, Apr. 2011.

[17] J.-H. Kim, J.-G. Kim, Y.-H. Ji, Y.-C. Jung, and C.-Y. Won, "An islanding detection method for a grid-connected system based on the Goertzel algorithm," *IEEE Trans. Power Electron,* vol. 26, no. 4, pp. 10491055, Apr. 2011.

[18] L. A. C. Lopes and Y. Zhang, "Islanding detection assessment of multiinverter systems with active frequency drifting methods," *IEEE Trans. Power Del.,* vol. 23, no. 1, pp. 480486, Jan. 2008.

[19] M. Khodaparastan, H. Vahedi, F. Khazaeli, and H. Oraee, "A novel hybrid islanding detection method for inverter-based DGs using SFS and ROCOF," *IEEE Trans. Power Del.,* 2015, to be published.

[20] P. Mahat, C. Zhe, and B. Bak-Jensen, "A hybrid islanding detection technique using average rate of voltage change and real power shift," *IEEE Trans. Power Del.,* vol. 24, no. 2, pp. 764771, Apr. 2009.

[21] J. C. M. Vieira, W. Freitas, Z. Huang, W. Xu, and A. Morelato, "Formulas for predicting the dynamic performance of ROCOF relays for embedded generation applications," *Proc. Inst. Elect. Eng., Gen., Transm. Distrib,* vol. 153, no. 4, pp. 399406, Jul. 2006.

[22] S. Alshareef, S. Talwar, and W. G. Morsi, "A new approach based on wavelet design and machine learning for islanding detection of distributed generation," *IEEE Trans. Smart Grid,* vol. 5, no. 4, pp. 15751583, Jul. 2014.

[23] S. R. Samantaray, K. El-Arroudi, G. Joos, and I. Kamwa, "A fuzzy rule-based approach for islanding detection in distributed generation," *IEEE Trans. Smart Grid,*vol. 25, no. 3, pp. 14271433, Jul. 2010.

[24] A. H. Mohammadzadeh Niaki and S. Afsharnia, "A new passive islanding detection method and its performance evaluation for multi-DG systems," *IEEE Trans. Smart Grid,*vol. 110, pp. 180187, May 2014.

[25] M. Bakhshi, R. Noroozian, and G. B. Gharehpetian, "Anti-islanding scheme for synchronous DG units based on TuftsKumaresan signal estimation method," *IEEE Trans. Power Del.,* vol. 28, no. 4, pp. 21852193, Oct. 2013.

[26] H. H. Zeineldin, T. A. Galil, E. F. E. Saadany, and M. M. A. Salam, "Islanding detection of grid connected distributed generators using TLS ESPRIT," *Int. J. Elect. Power Syst. Res.,*vol. 77, pp. 155162, Apr. 2006.

[27] Z. Lin, T. Xia, Y. Ye, Y. Zhang, L. Chen, Y. Liu, K. Tomsovic, T. Bilke, and F. Wen, "Application of wide area Measurement systems to islanding detection of bulk power systems," *IEEE Trans. Power Syst.,*vol. 28, no. 2, pp. 20062015, May 2013.

[28] IEEE Distribution Planning Working Group, "Radial distribution test feeders," *IEEE Trans. Power Syst.,*vol. 6, no. 3, pp. 975985, Aug. 1991.

[29] M. A. Refern, O. Usta, and G. Fielding, "Protection against loss of utility grid supply for a dispersed storage and generation unit," *IEEE Trans. Power Syst.,*vol. 8, no. 3, pp. 948-954, July 1993.

[30] M. A. Redfern, J. I. Barren, and O. Usta, "A new microprocessor based islanding protection algorithm for dispersed storage and generation, units," *IEEE Trans. Power Syst.,*vol. 10, no. 3, pp. 1249-1254, July.

[31] F. Pai, and S. Huang, "A detection algorithm for islanding-prevention of dispersed consumer-owned storage and generating units," *IEEE Trans. Energy Conversion,*vol. 16, no. 4, pp. 346-351, 2001.